

# NIRVANA: STRUCTURED PRUNING REIMAGINED FOR LARGE LANGUAGE MODELS COMPRESSION

**Mengting Ai, Tianxin Wei, Sirui Chen, Jingrui He**

University of Illinois Urbana-Champaign

{mai10, twei10, sirui6, jingrui}@illinois.edu

## ABSTRACT

Structured pruning of large language models (LLMs) offers substantial efficiency improvements by removing entire hidden units, yet current approaches often suffer from significant performance degradation, particularly in zero-shot settings, and necessitate costly recovery techniques such as supervised fine-tuning (SFT) or adapter insertion. To address these critical shortcomings, we introduce **NIRVANA**, a novel pruning method explicitly designed to balance immediate zero-shot accuracy preservation with robust fine-tuning capability. Leveraging a first-order saliency criterion derived from the Neural Tangent Kernel under Adam optimization dynamics, NIRVANA provides a theoretically grounded pruning strategy that respects essential model training behaviors. To further address the unique challenges posed by structured pruning, NIRVANA incorporates an *adaptive sparsity allocation* mechanism across layers and modules (attention vs. MLP), which adjusts pruning intensity between modules in a globally balanced manner. Additionally, to mitigate the high sensitivity of pruning decisions to calibration data quality, we propose a simple yet effective *KL divergence-based calibration data selection* strategy, ensuring more reliable and task-agnostic pruning outcomes. Comprehensive experiments conducted on Llama3, Qwen, and T5 models demonstrate that NIRVANA outperforms existing structured pruning methods under equivalent sparsity constraints, providing a theoretically sound and practical approach to LLM compression. The code is available at <https://github.com/iDEA-iSAIL-Lab-UIUC/NIRVANA>.

## 1 INTRODUCTION

Transformer-based (Vaswani et al., 2017) large language models (LLMs) have revolutionized natural language processing, achieving unprecedented performance across diverse tasks. However, this remarkable capability comes at the cost of enormous computational resources, making these models increasingly inaccessible to the broader community. For instance, a typical 7-billion-parameter model requires approximately 14GB of GPU memory at 16-bit precision, incurring prohibitive costs for training and inference. This computational barrier not only restricts widespread adoption but also impedes the democratization of AI, reinforcing misconceptions that advanced AI tools are inherently exclusive to resource-rich institutions (Ai et al., 2025a; Zou et al., 2024; Dang et al., 2025; Wei et al., 2023; Tian et al., 2025).

To alleviate this critical bottleneck, model compression techniques—particularly pruning (LeCun et al., 1989)—emerge as an essential strategy, aiming to create lighter, more accessible models without substantially compromising their effectiveness. Current pruning approaches generally fall into three categories: **(1) Unstructured pruning** methods (e.g., SparseGPT (Frantar and Alistarh, 2023), Wanda (Sun et al., 2023)<sup>1</sup>) achieve near-lossless zero-shot accuracy by removing individual weights (Frantar and Alistarh, 2023; Sun et al., 2023), but fail to deliver practical speedups due to irregular sparsity patterns incompatible with hardware accelerators (Cheng et al., 2024). **(2) Semi-structured pruning** (e.g., 2:4 block sparsity (Zheng et al., 2024)) addresses this limitation by enforcing fixed sparsity patterns optimized for NVIDIA sparse tensor cores (Yang et al., 2023). However, such approaches still struggle during supervised fine-tuning (SFT), as optimizer updates inevitably disrupt the predefined structures, limiting their end-to-end usability. **(3) Structured**

<sup>1</sup>These two can also be applied for semi-structured pruning.

**pruning** methods, such as LLM-Pruner (Ma et al., 2023) and FLAP (An et al., 2024), further improve hardware compatibility by removing entire neurons or layers, offering acceleration across both inference and training. Orthogonal to pruning, quantization further compresses models by reducing their numerical precision, presenting a similar dilemma between computational gains and performance preservation (Lin et al., 2024; Frantar et al., 2023; Xiao et al., 2023; Zhao et al., 2024).

While structured pruning holds the greatest promise for practical deployment, existing methods face several critical challenges: **(1) Inefficient recovery tuning lacking alignment with fine-tuning dynamics:** To recover from pruning-induced performance drops, existing methods rely heavily on costly fine-tuning procedures like LoRA adapters (Hu et al., 2021a) or extensive SFT (Xia et al., 2024). However, these recovery methods do not explicitly account for how pruning decisions influence the model’s fine-tuning capability, resulting in inefficient resource usage and sub-optimal results. **(2) Ignoring layer- and module-specific characteristics:** Current methods typically apply pruning uniformly across all layers or modules (attention and MLP), disregarding their distinct roles within the network. This oversight often results in suboptimal pruning choices, impairing model performance. **(3) Neglect of calibration data influence:** Pruning decisions depend critically on the calibration dataset used; yet, existing approaches rarely discuss or optimize this crucial factor, leaving pruning outcomes vulnerable to suboptimal data selection.

To address these critical gaps, we introduce **NIRVANA** (NTK-InfoRmed adaptiVe neuron & AttentioN heAd pruning), a novel structured pruning method that tightly integrates pruning decisions with model fine-tuning dynamics through the lens of the Neural Tangent Kernel (NTK) (Jacot et al., 2018). By aligning pruning criteria with the NTK spectrum under Adam—the de facto optimizer for LLMs—NIRVANA uniquely balances immediate accuracy preservation and long-term fine-tuning adaptability. Additionally, NIRVANA employs an adaptive sparsity allocation strategy across layers and modules, complemented by a calibration data selection mechanism based on KL divergence, making pruning both theoretically grounded and practically effective. Our primary contributions are:

- **NIRVANA:** A novel NTK-guided structured pruning method explicitly designed to preserve zero-shot accuracy while maintaining fine-tuning capability, connecting pruning decisions to fundamental training dynamics.
- An **adaptive sparsity allocation** strategy that dynamically adjusts pruning ratios across layers and modules, explicitly addressing overlooked disparities in existing pruning methodologies.
- A **KL-divergence-driven calibration data selection** strategy ensuring pruning robustness by identifying optimal subsets that minimize post-pruning output discrepancies, effectively decoupling pruning quality from calibration dataset size.
- **Comprehensive experiments** on prominent LLMs (Llama3 family, Qwen and T5) demonstrating that NIRVANA significantly outperforms state-of-the-art structured pruning methods in perplexity and downstream task accuracy under similar sparsity budgets, while seamlessly integrating into standard fine-tuning pipelines without requiring additional modifications.

## 2 RELATED WORK

**Unstructured and semi-structured pruning.** Recent unstructured pruning methods, such as SparseGPT (Frantar and Alistarh, 2023) and Wanda (Sun et al., 2023), prune individual weights using local criteria, but produce irregular sparsity patterns that are inefficient for current hardware. Semi-structured methods address this by imposing fixed patterns (e.g., 2:4 sparsity (Fang et al., 2024; Zheng et al., 2024)), yet still struggle to support efficient training and require specialized hardware.

**Structured pruning.** Structured pruning removes entire neurons, attention heads, or layers, enabling practical speedups. Methods such as LLM-Pruner (Ma et al., 2023), Sheared Llama (Xia et al., 2024), and SlimGPT (Ling et al., 2024) prune components based on local pruning scores (Lee et al., 2021; Salama et al., 2019), and typically treat attention and MLP uniformly, ignoring their distinct features. Recent approaches such as Adapt-Pruner (Wang et al., 2025), FLAP (An et al., 2024), and ShortGPT (Men et al., 2024) introduce global or layer-wise pruning strategies, yet do not explicitly address the imbalance between modules. SliceGPT (Ashkboos et al., 2024) applies PCA-based transformations per block, but remains highly sensitive to calibration data, reflecting a broader limitation: most methods overlook the influence of calibration data on pruning outcomes.

**Calibration data.** Pruning methods often depend on a small *calibration* set to estimate activation or gradient statistics for scoring and pruning decisions. Recent works (Williams and Aletras, 2024) highlight that the *selection* of calibration data plays a critical role in the pruning outcome, with factors such as data quality, diversity, and alignment with the model’s pretraining distribution shown to significantly influence pruning effectiveness (Bandari et al., 2024; Ji et al., 2024). A more detailed version of related work can be found in Section A.

### 3 PRELIMINARY & PROBLEM FORMULATION

#### 3.1 PRELIMINARY OF MODEL ARCHITECTURE AND NTK

We use lowercase letters to denote scalars, boldface lowercase letters to denote vectors, and boldface uppercase letters to denote matrices. The element-wise product is denoted by  $\odot$ . The neural network is denoted by  $f$ , parameterized by  $\mathbf{W}$ , and  $\mathbf{x}$  represents the input data. See the full notation in Table 4. Since most of the current LLMs are based on SwiGLU Shazeer (2020) structure, we focus on pruning the Attention & MLP sub-layer inside a SwiGLU Transformer block. For the MLP block, it is parameterized by three weight matrices:  $\mathbf{W}_{\text{gate}} \in \mathbb{R}^{d \times m}$ ,  $\mathbf{W}_{\text{up}} \in \mathbb{R}^{d \times m}$ , and  $\mathbf{W}_{\text{down}} \in \mathbb{R}^{m \times d}$ . For an input token  $\mathbf{x} \in \mathbb{R}^d$ , the MLP output is computed as:

$$\mathbf{H}(\mathbf{x}) = \left( \sigma(\mathbf{x}\mathbf{W}_{\text{gate}}) \odot \mathbf{x}\mathbf{W}_{\text{up}} \right) \mathbf{W}_{\text{down}},$$

where the activation function Swish  $\sigma(\cdot)$  is applied elementwise, and biases are omitted for simplicity (either because modern designs often exclude them or their contribution is marginal (Dubey et al., 2024)). As for the Multi-Head Attention (MHA) block with  $\mathbf{Q}_a = \mathbf{x}\mathbf{W}_a^Q$ ,  $\mathbf{K}_a = \mathbf{x}\mathbf{W}_a^K$ ,  $\mathbf{V}_a = \mathbf{x}\mathbf{W}_a^V$ ,  $a = 1, \dots, h$ , where  $\mathbf{W}_a^Q, \mathbf{W}_a^K, \mathbf{W}_a^V \in \mathbb{R}^{d \times d_h}$  and  $d_h = d/h$ , the attention for each head  $a$  is  $\text{head}_a = \text{softmax} \left( \frac{\mathbf{Q}_a \mathbf{K}_a^\top}{\sqrt{d_h}} \right) \mathbf{V}_a$ , and the MHA output <sup>2</sup> is

$$\text{MHA}(\mathbf{x}) = [\text{head}_1, \dots, \text{head}_h] \mathbf{W}^O, \quad \mathbf{W}^O \in \mathbb{R}^{hd_h \times d}.$$

Neural Tangent Kernel (NTK) (Jacot et al., 2018) provides a kernel-based framework for analyzing the training dynamics of neural networks by approximating their behavior as linear models in function space, particularly in the infinite-width limit. In our paper, we use Adam-based NTK with the form of

$$\Theta(\mathbf{x}, \mathbf{x}) = \nabla_{\mathbf{W}} f(\mathbf{x}; \mathbf{W}) \text{ sign}(\nabla_{\mathbf{W}} f(\mathbf{x}; \mathbf{W}))^\top = \langle \nabla_{\mathbf{W}} f(\mathbf{x}; \mathbf{W}), \text{sign}(\nabla_{\mathbf{W}} f(\mathbf{x}; \mathbf{W})) \rangle.$$

See the details of the derivation in Section A.6

#### 3.2 PROBLEM FORMULATION OF PRUNING PROCESS

We assume that the output  $f(\mathbf{x}; \mathbf{W})$  is a single value, which is common in classification or next-token generation tasks.<sup>3</sup> Given a sparsity level  $v$ , the target of pruning can be then written in the form of:

$$\text{argmin}_{\hat{\mathbf{W}}, \mathbf{M}} \mathcal{L} \left( f(\mathbf{x}; \mathbf{W}), f(\mathbf{x}; \hat{\mathbf{W}} \odot \mathbf{M}) \right),$$

where  $\mathbf{M}$  is the mask matrix that has the same shape as  $\mathbf{W}$ . Directly solving this joint optimization over  $\hat{\mathbf{W}}$  and  $\mathbf{M}$  is NP-hard. Consequently, popular practices include fixing the weights (i.e., setting  $\hat{\mathbf{W}} = \mathbf{W}$ ) and searching for  $\mathbf{M}$  only (one-shot pruning (Frankle and Carbin, 2019; Frantar and Alistarh, 2023; Sun et al., 2023; Chen et al., 2021)), or selecting  $\mathbf{M}$  first and then optimizing  $\hat{\mathbf{W}}$ , which typically requires further fine-tuning or re-training (Kwon et al., 2022; Ma et al., 2023). General pruning approaches define a *saliency score*  $S_{i,j}$  for each weight, which estimates the impact of removing the connection  $\mathbf{W}_{i,j}$ . A general form of the saliency score is:

$$S_{i,j} = \frac{\partial \mathcal{I}}{\partial \mathbf{W}_{i,j}} \cdot \mathbf{W}_{i,j}, \quad (1)$$

<sup>2</sup>In Llama3’s implementation, which employs Grouped Query Attention (GQA), multiple query heads share the same key-value (KV) head. When calculating group saliency scores, we align query (Q) and output (O) heads with their corresponding KV head groupings through index mapping.

<sup>3</sup>Without loss of generality, our analysis can be extended to the vector-output case.

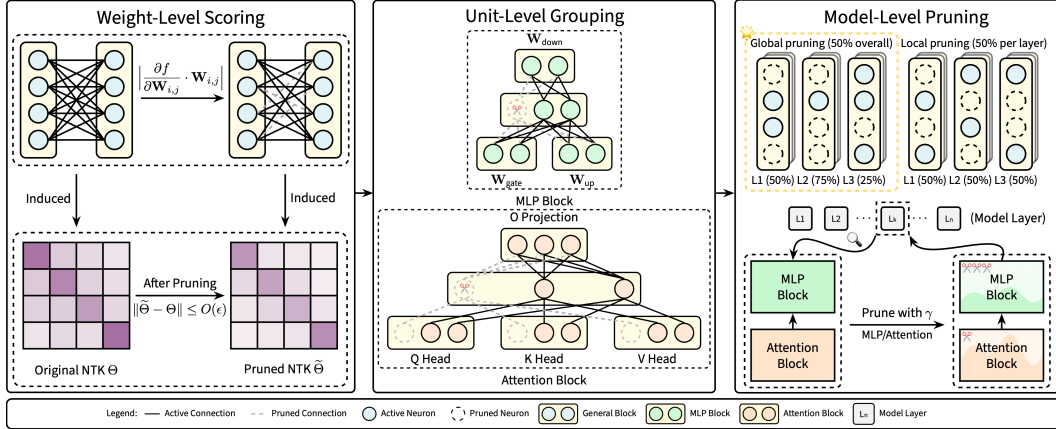


Figure 1: Illustration of our proposed **NIRVANA** framework. Left: We compute weight-level saliency scores using the NTK-guided score. Middle: We aggregate the scores into structured units. Right: We perform global pruning with an adaptive sparsity allocation strategy that adjusts pruning ratios both across layers and between MLP and attention modules with  $\gamma$ .

where  $\mathcal{I}$  is a function that measures the importance of the weight  $\mathbf{W}$  to the network  $f$ . Once these scores are computed, the mask is obtained by selecting the top  $\kappa\%$  of weights:

$$\mathbf{M}_{i,j} = \text{Top}_\kappa(S)_{i,j} = \begin{cases} 1, & \text{if } S_{i,j} \text{ is among the top } \kappa\%, \\ 0, & \text{otherwise.} \end{cases}$$

This binary mask is then applied to the weights for pruning.

## 4 PROPOSED METHOD: NIRVANA

In this section, we present the details of NIRVANA. The corresponding pseudocode is provided in Algorithm 1, and an illustrative diagram is shown in Figure 1. Our method is built around four core components, each addressing a different level of the pruning process:

- **Weight-level saliency scoring:** quantifying the importance of individual weights based on their impact on the model’s output (Section 4.1).
- **Structured grouping at the neuron/head level:** aggregating weight saliencies into group-wise scores for MLP neurons and attention heads to enable structured pruning (Section 4.2).
- **Adaptive sparsity allocation at the model level:** applying a global sparsity strategy and balancing pruning between MLP and attention via the adaptive ratio  $\gamma$  (Section 4.3).
- **Calibration data selection:** identifying high-quality calibration data that provides the most informative gradients for reliable pruning (Section 4.4).

### 4.1 SALIENCY SCORE AND ITS CONNECTION TO NTK - WEIGHT LEVEL

We begin by deriving the saliency score, quantifying the *importance* of a weight in terms of its direct impact on the model output, i.e.  $\mathcal{I} = f(\mathbf{x}; \mathbf{W})$ , where  $f(\mathbf{x}; \mathbf{W})$  denote the network output for input  $\mathbf{x}$  and weights  $\mathbf{W}$ . Consider removing a single weight  $\mathbf{W}_{i,j}$  by setting it to zero while keeping all other weights unchanged. We define the perturbation as:  $\Delta \mathbf{W} = -\mathbf{W}_{i,j}$ , so that the new weight matrix becomes:  $\mathbf{W}' = \mathbf{W} + \Delta \mathbf{W}$ , where  $\Delta \mathbf{W}$  is zero everywhere except at entry  $(i, j)$ . The resulting change in output is:  $\Delta f = f(\mathbf{x}; \mathbf{W}') - f(\mathbf{x}; \mathbf{W})$ . Applying a first-order Taylor expansion around  $\mathbf{W}$ , we obtain:  $f(\mathbf{x}; \mathbf{W} + \Delta \mathbf{W}) \approx f(\mathbf{x}; \mathbf{W}) + \frac{\partial f}{\partial \mathbf{W}_{i,j}} \Delta \mathbf{W}_{i,j}$ , which is simplified to:

$$\Delta f \approx -\frac{\partial f(\mathbf{x}; \mathbf{W})}{\partial \mathbf{W}_{i,j}} \mathbf{W}_{i,j}.$$

Thus, the change in output when pruning  $\mathbf{W}_{i,j}$  is approximately proportional to its gradient scaled by its magnitude. We define the saliency score as the absolute value of this first-order effect:

$$S(\mathbf{W}_{i,j}) = \left| \frac{\partial f(\mathbf{x}; \mathbf{W})}{\partial \mathbf{W}_{i,j}} \cdot \mathbf{W}_{i,j} \right|. \quad (2)$$

This score quantifies how much the output is expected to change if the weight is pruned, providing a principled criterion for pruning decisions. As illustrated in Figure 1 (left), our method begins by computing weight-level saliency scores using the proposed NTK-guided criterion, which not only quantifies the immediate output perturbation but also implicitly ensures NTK stability.

**Bridging to the training dynamics via NTK.** While our saliency score in Equation (2) quantifies immediate, first-order changes to the model’s outputs, it does not directly inform how pruning affects the model’s longer-term training behavior. Ideally, pruning decisions should not only minimize immediate output degradation but also preserve the model’s behavior during fine-tuning. Unlike prior work that relies on empirical fine-tuning to recover performance Ma et al. (2023); Ashkboos et al. (2024), we introduce the NTK, a powerful theoretical tool capturing the training dynamics of neural networks, to provide a theoretical insight. The NTK characterizes how a model’s predictions evolve under gradient-based updates, effectively encoding the sensitivity of outputs to parameter changes across training steps. If the NTK remains stable post-pruning, the pruned model preserves a similar optimization trajectory, ensuring efficient recovery of performance through fine-tuning. Recall the NTK for input  $\mathbf{x}$  is defined as:

$$\Theta(\mathbf{x}, \mathbf{x}) = \langle \nabla_{\mathbf{W}} f(\mathbf{x}; \mathbf{W}), \text{sign}(\nabla_{\mathbf{W}} f(\mathbf{x}; \mathbf{W})) \rangle,$$

where the gradient  $\nabla_{\mathbf{W}} f(\mathbf{x}; \mathbf{W})$  reflects the sensitivity of the model output with respect to each parameter. For a given weight  $\mathbf{W}_{i,j}$ , its contribution to the NTK is proportional to  $|\partial f / \partial \mathbf{W}_{i,j}|$ . However, relying solely on sensitivity is insufficient to assess the true impact of pruning, as it ignores the current contribution of the weight itself to the output. Consider two weights:  $\mathbf{W}_{i,j}$  with a large magnitude but a small gradient, and  $\mathbf{W}_{i',j'}$  with a small magnitude but a large gradient. Pruning  $\mathbf{W}_{i,j}$  may cause significant output distortion due to its large weight, despite its small gradient; in contrast, pruning  $\mathbf{W}_{i',j'}$  would induce substantial changes in the NTK, as the gradient term dominates, even if its immediate contribution to the output is minor. This illustrates the need to balance both the parameter value and its sensitivity to avoid disrupting either the output or the training dynamics captured by the NTK. Accordingly, our saliency score incorporates both aspects, ensuring that pruning decisions simultaneously minimize output perturbations and preserve NTK stability. We formalize this intuitive connection with the following NTK stability bound:

**Proposition 4.1** (Short version of Theorem E.1). *For a Transformer model pruned with NIRVANA, let  $\tilde{\Theta}$  denote the NTK after pruning. For sufficiently small  $\epsilon > 0$ , we have:*

$$\|\tilde{\Theta} - \Theta\| \leq O(\epsilon). \quad (3)$$

This result justifies that pruning based on the saliency score in (2) preserves both immediate model outputs (via first-order Taylor approximation) and long-term fine-tuning potential (via NTK stability). As a result, NIRVANA achieves both strong zero-shot approximation and robust fine-tuning recovery.

#### 4.2 STRUCTURED PRUNING VIA GROUPING OF HIDDEN UNITS - NEURON/ATTENTION HEAD LEVEL

After obtaining the saliency score for each weight, we need to group them in order to achieve practical efficiency gains for structured pruning. By pruning at the granularity of entire hidden units—such as MLP neurons and attention heads—our method directly reduces the model’s computational dimensions. We perform this by grouping weights according to hidden units—a strategy that aligns with the dependency graph approach in (Fang et al., 2023). In the MLP sub-layer, we treat each hidden unit  $u \in \{1, \dots, m\}$  as a group, which consists of all weights in the  $u$ -th column of  $\mathbf{W}_{\text{gate}}$  and  $\mathbf{W}_{\text{up}}$ , and the  $u$ -th row of  $\mathbf{W}_{\text{down}}$ . For each hidden unit, we compute a cumulative saliency score by summing the saliency scores of its associated weights:

$$S(u) = \sum_{i=1}^d \left| \frac{\partial f}{\partial (\mathbf{W}_{\text{gate}})_{i,u}} \cdot (\mathbf{W}_{\text{gate}})_{i,u} \right| + \sum_{i=1}^d \left| \frac{\partial f}{\partial (\mathbf{W}_{\text{up}})_{i,u}} \cdot (\mathbf{W}_{\text{up}})_{i,u} \right| + \sum_{i=1}^d \left| \frac{\partial f}{\partial (\mathbf{W}_{\text{down}})_{u,i}} \cdot (\mathbf{W}_{\text{down}})_{u,i} \right|.$$

For MHA, we aggregate the scores for each attention head  $a$ , which consists of all weights in  $\mathbf{W}_a^Q, \mathbf{W}_a^K, \mathbf{W}_a^V$  and the corresponding part  $\mathbf{W}^O[a] \in \mathbb{R}^{d_h \times d}$ :

$$S(a) = \sum_{i=1}^d \sum_{j=1}^{d_h} \left| \frac{\partial f}{\partial (\mathbf{W}_a^Q)_{i,j}} \cdot (\mathbf{W}_a^Q)_{i,j} \right| + \sum_{i=1}^d \sum_{j=1}^{d_h} \left| \frac{\partial f}{\partial (\mathbf{W}_a^K)_{i,j}} \cdot (\mathbf{W}_a^K)_{i,j} \right| \\ + \sum_{i=1}^d \sum_{j=1}^{d_h} \left| \frac{\partial f}{\partial (\mathbf{W}_a^V)_{i,j}} \cdot (\mathbf{W}_a^V)_{i,j} \right| + \sum_{i=1}^{d_h} \sum_{j=1}^d \left| \frac{\partial f}{\partial (\mathbf{W}^O[a])_{i,j}} \cdot (\mathbf{W}^O[a])_{i,j} \right|$$

After computing these scores, we rank all hidden units by their aggregated saliency scores. Units falling below a global threshold (determined by our target sparsity level  $v$ , detailed further in Section 4.3) are pruned. Specifically, this involves zeroing out the corresponding column in  $\mathbf{W}_{\text{gate}}$  and  $\mathbf{W}_{\text{up}}$ , the corresponding row in  $\mathbf{W}_{\text{down}}$ , and the entire attention head  $a$ . This grouping-based pruning ensures that the network's dependency structure is respected and that entire units are removed together, leading to real efficiency gains. See Figure 1 (middle) for a visual illustration.

#### 4.3 ADAPTIVE SPARSITY ALLOCATION BETWEEN ATTENTION AND MLP - MODEL LEVEL

Having established the unit-level saliency scores, we now address model-level pruning, focusing on how units are ranked globally and how sparsity is allocated between MLP neurons and attention heads. Most prior works (Sun et al., 2023; Frantar and Alistarh, 2023; Ma et al., 2023; Ashkboos et al., 2024; Ling et al., 2024) adopt local sparsity strategies by applying fixed pruning ratios to each layer or module, implicitly treating all units equally regardless of their functional role. However, recent studies (Wang et al., 2025; An et al., 2024) have also noted the challenge of balancing pruning across modules due to scale mismatches, though their approaches primarily rely on heuristic metric normalization. In contrast, we adopt a principled global sparsity strategy where all units across layers and modules are ranked jointly by their saliency scores, ensuring the overall sparsity target is achieved. To prevent layer collapse (Tanaka et al., 2020; Vysogorets and Kempe, 2023), we introduce a simple safeguard that retains at least one unit per layer.

Furthermore, motivated by prior observations that MLP layers tend to store factual knowledge more efficiently than attention heads (Nichani et al., 2024), we introduce an explicit sparsity allocation parameter  $\gamma$  to control the relative pruning rates between MLP neurons and attention heads. Unlike heuristic standardization, this parameterized allocation allows us to systematically adjust pruning aggressiveness between the two components, providing a more flexible and interpretable balance:

$$v_{\text{Attn}} = \frac{v(\#\text{MLP} + \#\text{Attn})}{\#\text{Attn} + \gamma \cdot \#\text{MLP}}, \quad v_{\text{MLP}} = \gamma \cdot v_{\text{Attn}}, \quad (4)$$

where  $v$  denotes the overall target sparsity,  $v_{\text{MLP}}$  and  $v_{\text{Attn}}$  denote the applied sparsity to MLP neurons and attention heads, respectively, and  $\#\text{MLP}$  and  $\#\text{Attn}$  represent their total parameter counts. Details on how  $\gamma$  is determined are provided in Section F. This global ranking and adaptive allocation process is illustrated in Figure 1 (right).

#### 4.4 CALIBRATION DATA SELECTION VIA KL DIVERGENCE

As pruning transitions from individual weights as in Equation (2) to larger groups (neurons/heads), the variance in the aggregated saliency scores across these groups can be more pronounced compared to weight-level pruning. This makes it critical to carefully select calibration data that accurately reflects the model's behavior. Existing works (Williams and Aletras, 2024; Bandari et al., 2024; Ji et al., 2024) observe that the quality and diversity of the calibration data are critical to the effectiveness of pruning. However, in our experiments, we find that the quality or diversity of the calibration data does not consistently correlate with model performance, as illustrated by examples in Section G. We also empirically observe that neither the length nor the quantity of calibration data directly correlates with the performance. Therefore, we adopt a lightweight yet effective approach to select calibration data. We propose using the KL divergence to measure the output discrepancy between the pruned model  $\hat{f}$  and the original model  $f$ , serving as a proxy for selecting calibration data. Minimizing KL divergence ensures calibration data induces pruning decisions that preserve the original model's output

distribution, avoiding biased gradients from unrepresentative samples. We define the calibration dataset  $\mathcal{C}^*$  as:

$$\mathcal{C}^* = \arg \min_{\substack{\mathcal{C} \subset \mathcal{D} \\ |\mathcal{C}|=n}} \frac{1}{n} \sum_{\mathbf{x} \in \mathcal{C}} \text{KL}(f(\mathbf{x}) \| \hat{f}(\mathbf{x})).$$

In detail, we randomly sample multiple candidate batches from the dataset and prune the model using each candidate batch as calibration data. For each pruned model, we compute the KL divergence on a fixed held-out evaluation set. The batch that yields the lowest KL divergence is selected as the calibration data  $\mathcal{C}^*$ . Since each pruning round requires only a single backward pass and is performed on a small subset, the overall process remains efficient and incurs minimal additional computational overhead. The pseudocode of this process can be found in Algorithm 2.

## 5 EXPERIMENTS

We begin by outlining the experimental setup, followed by comparative evaluations against several baselines on Llama3.1-8B, conclude with an ablation study. Additional experiments on Llama3.2-3B, Qwen2.5-7B, and fine-tuning on T5-base are provided in Section B.1, Section B.2, and Section B.3, along with efficiency analysis in Section B.4.

### 5.1 EXPERIMENTAL SETTINGS

**Model backbones.** We evaluate NIRVANA on three open-source large language models covering both decoder-only and encoder-decoder architectures: Llama3.1-8B, Llama3.2-3B (Dubey et al., 2024), Qwen2.5-7B (et al., 2025), and T5-base (Raffel et al., 2023). Our main experiments are conducted on Llama3.1-8B, with additional results for the other models provided in Section B.

**Baselines.** We compare NIRVANA with several state-of-the-art structured pruning baselines, including LLM-Pruner (Ma et al., 2023), SliceGPT (Xia et al., 2024), and FLAP (An et al., 2024). For LLM-Pruner, we use the `param_second` configuration, which we find performs better in our setting. All methods are compared at matched target model sizes for fairness.

**Evaluation tasks and datasets.** To comprehensively evaluate the effectiveness of our method, we conduct experiments on three types of tasks. First, we follow (Ma et al., 2023) to evaluate zero-shot perplexity on WikiText2 (Merity et al., 2016), PTB (Wagner et al., 2020), and Lambada (Paperno et al., 2016). Second, we evaluate zero-shot accuracy on a suite of commonsense reasoning benchmarks, including ARC-easy (Clark et al., 2018), Winogrande (Sakaguchi et al., 2021), and HellaSwag (Zellers et al., 2019), as well as SVAMP (math word problem) (Patel et al., 2021). Additionally, we assess 3-shot Pass@1 performance on MBPP (code generation) (Austin et al., 2021), all except SVAMP use the `lm-eval-harness` (Gao et al., 2024) framework. Finally, we conduct recovery tuning experiments using LoRA (Hu et al., 2021b) on Alpaca (Taori et al., 2023) following (Ma et al., 2023). All experiments are run on NVIDIA A100-SXM4-40GB GPUs.

**Calibration data.** All methods, except SliceGPT, use 32 samples from BookCorpus with a sequence length of 128 as calibration data to preserve the zero-shot setting. For SliceGPT, we follow the original setup using 128 samples from WikiText with a sequence length of 2048, as using BookCorpus leads to significant performance degradation.

### 5.2 RESULTS ON LLAMA3.1-8B

Table 1 summarizes the evaluation results across various sparsity levels and benchmarks. Overall, NIRVANA consistently outperforms existing pruning baselines, with the performance gap widening notably under higher sparsity. This demonstrates the effectiveness of our approach in maintaining model capabilities while enabling aggressive compression.

Among the tasks, MBPP—a challenging code generation benchmark—highlights the limitations of existing methods, where most baselines fail to produce usable models with near-zero pass rates. In contrast, NIRVANA retains significantly better performance, indicating its ability to preserve generative capabilities beyond general language modeling metrics. The performance gap between NIRVANA and the baselines widens as the sparsity ratio increases. At lower sparsity levels, LLM-Pruner’s local magnitude-based scoring remains effective in preserving key weights, as the pruning

Table 1: Evaluation results of Llama3.1-8B. **Bold** indicates the best results while underline indicates the second-best. We report both the zero-shot results and the performance after recovery fine-tuning. The down-arrow notation ( $\downarrow$ ) indicates that a lower metric represents better performance. The results are obtained through three runs.

Sparsity	Method	WikiT $\downarrow$	PTB $\downarrow$	LambD $\downarrow$	ARC-e	WinoG	HellaS	SVAMP	MBPP*	Avg	#Param
0%	Llama3.1-8B	8.50	14.02	20.09	81.52	73.56	78.90	72.67	48.60	71.05	8.03B
20%	LLM-Pruner	<u>17.45</u>	<u>27.89</u>	<u>28.33</u>	<b>69.57</b>	66.06	65.89	<u>22.33</u>	<u>4.40</u>	<u>45.65</u>	6.73B
	SliceGPT	21.10	118.79	252.46	53.70	61.61	51.40	0.00	0.00	33.34	6.57B
	FLAP	20.88	31.35	31.72	60.35	<u>66.22</u>	59.03	16.33	3.40	41.07	6.61B
	NIRVANA (ours)	<b>13.38</b>	<b>19.77</b>	<b>26.20</b>	<u>68.52</u>	<b>67.40</b>	<b>66.75</b>	<b>49.00</b>	<b>23.80</b>	<b>55.09</b>	6.62B
w/ tune	LLM-Pruner	<u>12.57</u>	<u>19.77</u>	<b>25.00</b>	<b>74.92</b>	<b>68.27</b>	74.06	33.33	<u>25.20</u>	<u>55.16</u>	6.75B
	SliceGPT	49.81	87.25	81.64	61.53	61.56	59.91	0.00	0.60	36.72	6.58B
	FLAP	16.14	25.00	<u>30.63</u>	70.71	63.54	67.58	<u>34.33</u>	15.00	50.23	6.63B
	NIRVANA (ours)	<b>12.37</b>	<b>18.58</b>	<b>25.00</b>	<b>76.98</b>	<u>66.54</u>	<b>74.36</b>	<b>56.67</b>	<b>33.00</b>	<b>61.51</b>	6.64B
40%	LLM-Pruner	98.86	196.62	105.24	37.00	51.93	32.18	<u>11.33</u>	0.00	26.49	5.27B
	SliceGPT	61.63	421.14	647.20	35.61	50.99	32.20	0.00	0.00	23.76	5.44B
	FLAP	45.44	<u>69.02</u>	<u>49.23</u>	<u>42.85</u>	<b>58.72</b>	43.60	9.66	0.00	30.97	5.22B
	NIRVANA (ours)	<b>28.33</b>	<b>38.72</b>	<b>43.19</b>	<u>45.79</u>	<u>58.33</u>	<b>45.85</b>	<u>11.67</u>	<b>2.20</b>	<u>32.77</u>	5.23B
w/ tune	LLM-Pruner	33.12	74.63	59.96	56.90	53.59	51.51	11.67	0.20	34.77	5.29B
	SliceGPT	156.76	224.54	214.26	48.19	53.83	43.68	0.00	0.00	29.14	5.44B
	FLAP	<u>20.09</u>	<u>30.63</u>	<u>32.60</u>	<u>58.80</u>	<b>61.17</b>	<u>57.33</u>	<u>20.33</u>	<u>5.80</u>	<u>40.69</u>	5.25B
	NIRVANA (ours)	<b>19.17</b>	<b>27.45</b>	<b>31.64</b>	<b>62.33</b>	<u>57.93</u>	<b>58.74</b>	<u>22.33</u>	<b>11.00</b>	<u>42.47</u>	5.25B
50%	LLM-Pruner	215.94	356.02	196.62	31.19	49.01	28.82	7.33	0.00	23.27	4.55B
	SliceGPT	93.24	612.76	870.90	32.37	49.57	29.70	0.00	0.00	22.33	4.57B
	FLAP	68.21	<u>97.71</u>	<b>61.87</b>	<u>36.45</u>	<u>53.56</u>	<u>37.20</u>	<u>8.33</u>	0.00	<u>27.11</u>	4.50B
	NIRVANA (ours)	<b>48.94</b>	<b>67.95</b>	70.11	<b>37.54</b>	<b>54.38</b>	<b>37.72</b>	<u>9.33</u>	<b>0.20</b>	<b>27.83</b>	4.51B
w/ tune	LLM-Pruner	45.26	92.87	70.12	48.32	52.41	43.51	4.67	0.00	29.78	4.55B
	SliceGPT	198.93	246.61	248.55	40.19	52.49	36.57	0.00	0.00	25.85	4.59B
	FLAP	<u>28.33</u>	<u>42.52</u>	<u>43.87</u>	<u>50.76</u>	<b>58.09</b>	<u>49.90</u>	<u>15.67</u>	0.00	<u>34.88</u>	4.52B
	NIRVANA (ours)	<b>25.79</b>	<b>36.94</b>	<b>42.52</b>	<b>57.49</b>	<u>56.27</u>	<b>49.91</b>	<b>23.00</b>	<b>3.40</b>	<b>38.01</b>	4.53B

\* Pass@1. 3-shot.

ratio is modest and most important weights can still be retained. In contrast, the advantages of NIRVANA become more pronounced only at higher compression rates, where local heuristics struggle to capture the long-range dependencies and interactions across layers and modules. We also observe that methods like SliceGPT are highly sensitive to calibration data choices, leading to unstable performance across datasets. Notably, while FLAP’s global pruning strategy is competitive at high sparsity levels (40% and 50%), its performance degrades significantly at low sparsity (20%). This stands in sharp contrast to NIRVANA, which consistently achieves state-of-the-art results across all evaluated sparsity ratios. These results collectively validate the design choices of NIRVANA, including our NTK-guided scoring, adaptive sparsity allocation, and calibration data selection. Additional experiments on varying model sizes (Llama3.2-3B), model families (Qwen), and model architectures (T5-base) further support our findings; see Section B for details.

### 5.3 ABLATION STUDY

Our method includes several key components: (1) an NTK-inspired salience score; (2) an adaptive sparsity allocation strategy that combines global sparsity ranking with the pruning ratio  $\gamma$  to balance MLP units and attention heads; and (3) a calibration data selection strategy. We conduct an ablation study to assess the effects of these components, as shown in Table 2. Specifically, we compare NIRVANA with magnitude scoring, local pruning, without different ratio between MLP and attention ( $\gamma = 1$ ), and without KL-selected calibration data. We find that using magnitude-based scores for pruning leads to extreme performance collapse, highlighting the inadequacy of naive importance metrics in the LLM pruning context. Similarly, applying local

Table 2: Ablation study on Llama3.1-8B with 50% sparsity on three PPL datasets.

	Wikitext	PTB	Lambada
NIRVANA	48.94	70.11	70.11
Magnitude score	$\approx 10^6$	$\approx 10^5$	$\approx 10^6$
local	90.01	142.85	132.42
w/o ratio $\gamma$	102.00	139.42	123.04
w/o selected data	72.33	115.58	95.82

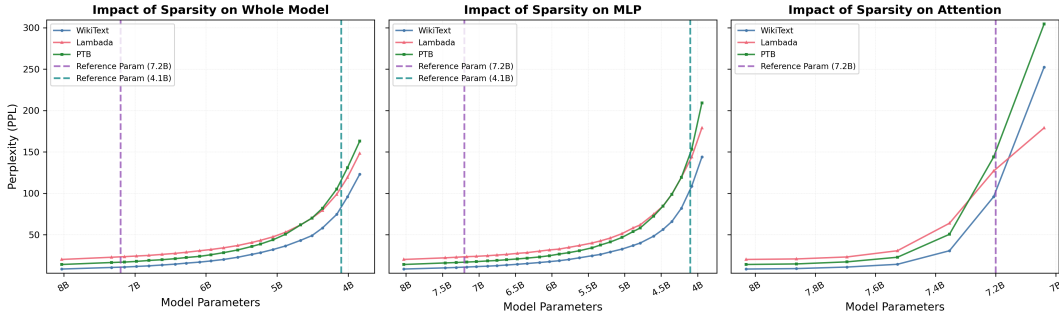


Figure 2: Comparison of pruning impact on perplexity across different pruning scopes. We evaluate pruning applied to the entire model, MLP modules only, and attention heads only. Dashed vertical lines indicate selected reference parameter points (7.2B and 4.1B) for visual comparison.

pruning instead of global pruning also leads to a performance drop, likely due to its inability to account for cross-layer importance differences.

**Impact of  $\gamma$ .** To better understand the impact of  $\gamma$ , we further investigate the impact of pruning scope by analyzing how perplexity changes as a function of the remaining model parameters. Figure 2 presents a detailed comparison where pruning is applied only to attention heads, only to MLP units, or jointly across the whole model using our proposed global strategy. We observe that perplexity degradation accelerates non-linearly as the model is pruned, following a near-exponential curve. This trend is particularly severe when pruning is limited to the attention module, which, despite its relatively small parameter footprint, plays an essential role in modeling long-range dependencies. Consequently, pruning attention heads alone quickly leads to catastrophic performance collapse at high sparsity levels. On the other hand, pruning only the MLP modules results in a more stable curve; however, it still exhibits rapid perplexity increase as the remaining parameters drop below critical thresholds (see the reference line of 4.1B). In contrast, the perplexity curves under NIRVANA are noticeably smoother, and at the same parameter budget, our approach consistently outperforms both MLP-only and attention-only pruning strategies. These results highlight the importance of balancing pruning across different components to mitigate bottlenecks and maintain overall model robustness.

**Calibration data selection.** We use calibration data from BookCorpus to maintain the zero-shot setting, with 32 examples of length 128 tokens. Our observations indicate that the pruned model’s performance is more sensitive to the quality of the calibration data than to its size or length, see Section G. Additionally, since calibration data is selected using a random seed and the pruning search process is repeated multiple times, keeping the data size small improves search efficiency. To identify optimal calibration data, we use the KL divergence between the pruned model and the original model as a proxy: specifically, we first prune the model using calibration data sampled with a random seed, then evaluate the KL divergence on a fixed validation set (also from BookCorpus) between the original and pruned models. We also test the pruned model on three perplexity benchmarks: WikiText, LAMBADA, and PTB, to assess whether performance correlates with the KL value. As shown in Figure 3, we observe a roughly linear relationship between KL divergence and downstream performance. Based on this, we select the calibration data that yields the smallest KL value for subsequent experiments.

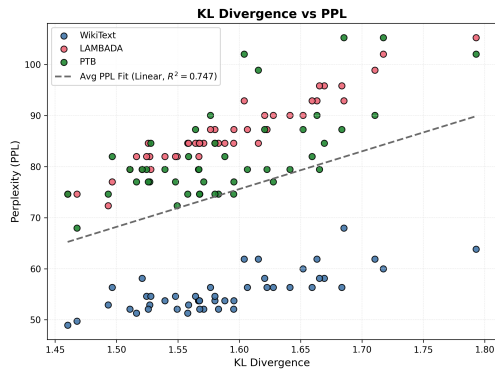


Figure 3: Relationship between KL divergence and perplexity (PPL) across different datasets over 50 runs. The observed linear correlation supports the effectiveness of using KL divergence as a proxy for data selection in pruning calibration.

Table 3: Post-pruning statistics during inference, tested on 20 rounds of Wikitext (batch size 32).

Sparsity	Method	#Param	FLOPs (G)	Latency (s/batch) ↓	Throughput (tok/s) ↑	Mem (GB)
0%	Llama3.1-8B	8.03B	6.98	0.33	12412.12	17.95
	LLM-Pruner	6.73B	5.75	0.41	9990.24	15.46
	SliceGPT	6.57B	5.59	0.38	10736.57	15.54
	FLAP	6.61B	5.56	0.50	8192.00	15.33
20%	NIRVANA	6.62B	5.61	0.28	14628.57	15.29
	LLM-Pruner	5.27B	4.42	0.52	7876.92	12.52
	SliceGPT	5.44B	4.21	0.31	13429.51	12.30
	FLAP	5.22B	4.19	0.39	10502.56	12.73
40%	NIRVANA	5.23B	4.26	0.23	17808.70	12.65
	LLM-Pruner	4.55B	3.76	0.20	20480.00	10.95
	SliceGPT	4.57B	3.52	0.27	15340.82	10.53
	FLAP	4.50B	3.52	0.30	13653.33	11.32
50%	NIRVANA	4.51B	3.55	0.21	19504.76	11.27

#### 5.4 EFFICIENCY ANALYSIS

**Inference Efficiency.** To evaluate the practical performance gains of structured pruning, we benchmark the inference efficiency of all methods on a single NVIDIA A100 GPU. The comprehensive results, including parameter counts, FLOPs, latency, throughput, and peak memory usage, are presented in Table 3. A key observation is the stark difference in how theoretical parameter reduction translates into practical speedups. While all methods successfully reduce peak memory usage, their impact on latency and throughput varies significantly. NIRVANA demonstrates a consistent and predictable trend: as sparsity increases, latency steadily decreases, and throughput improves accordingly. In sharp contrast, baseline methods like LLM-Pruner *exhibit erratic and non-monotonic behavior*. For instance, LLM-Pruner’s latency unexpectedly deteriorates from 0.33s to 0.52s at 40% sparsity, despite a 34% reduction in parameters. This suggests that merely reducing FLOPs is insufficient for guaranteed acceleration.

We hypothesize that this speed fluctuation is caused by pruning model dimensions into sizes that are incompatible with hardware optimizations. Modern GPUs achieve maximum throughput by leveraging specialized compute kernels (e.g., NVIDIA’s Tensor Cores), which are highly optimized for matrix operations where dimensions are multiples of 8 (Sarge et al., 2019; NVIDIA Corporation). When a layer’s dimension is not a multiple of 8, the GPU resorts to slower, general-purpose kernels, nullifying the benefits of sparsity and leading to performance degradation. Please refer to Section B.4 for the detailed analysis. Armed with this critical insight, we designed NIRVANA to be explicitly **hardware-aware**. Our pruning algorithm incorporates a dimension alignment step, which ensures that all remaining hidden dimensions after pruning are guaranteed to be multiples of 8. This deliberate design choice bridges the gap between theoretical sparsity and practical efficiency. As evidenced by our results, this hardware-aware approach allows NIRVANA to fully capitalize on the reduced model size, delivering robust and consistent acceleration where other methods falter. This finding underscores the importance of a hardware-software co-design approach for effective structured pruning.

## 6 CONCLUSION

We introduced **NIRVANA**, a novel structured pruning approach guided by the NTK, aiming to balance zero-shot accuracy preservation with fine-tuning adaptability. By explicitly linking the pruning criterion to NTK dynamics under Adam optimization, NIRVANA ensures pruning decisions that maintain both immediate output stability and fine-tuning recovery. Furthermore, our method integrates an adaptive sparsity allocation mechanism and a KL-divergence-based calibration data selection strategy, enhancing pruning robustness and efficiency. Extensive experiments demonstrate that NIRVANA consistently outperforms existing structured pruning baselines in both perplexity and downstream task performance under equivalent sparsity.

**Limitations.** While effective, NIRVANA still presents limitations. In particular, although our calibration data selection minimizes output KL divergence, the exact data properties that contribute to effective pruning remain unclear and deserve further investigation. Moreover, our approach relies on first-order approximations via NTK, and future work may explore higher-order dynamics. Lastly, our experiments focus on standard dense transformer architectures; extending NIRVANA to more complex settings like Mixture-of-Experts (MoE) (Ai et al., 2025b) is a promising direction.

**Broader impacts.** As a model compression method, NIRVANA primarily targets reducing the resource demands of large language models without altering their behavior or capabilities. We do not foresee direct societal risks or misuse arising uniquely from this work. However, as with any efficiency technique, care should be taken to ensure that improved accessibility to large models does not inadvertently facilitate harmful or unintended applications.

## REFERENCES

Mengting Ai, Tianxin Wei, Yifan Chen, Zeming Guo, and Jingrui He. Mlp fusion: Towards efficient fine-tuning of dense and mixture-of-experts language models, 2025a. URL <https://arxiv.org/abs/2307.08941>.

Mengting Ai, Tianxin Wei, Yifan Chen, Zhichen Zeng, Ritchie Zhao, Girish Varatkar, Bita Darvish Rouhani, Xianfeng Tang, Hanghang Tong, and Jingrui He. Resmoe: Space-efficient compression of mixture of experts llms via residual restoration. In *Proceedings of the 31st ACM SIGKDD Conference on Knowledge Discovery and Data Mining V.1*, KDD '25, page 1–12, New York, NY, USA, 2025b. Association for Computing Machinery. ISBN 9798400712456. doi: 10.1145/3690624.3709196. URL <https://doi.org/10.1145/3690624.3709196>.

Yongqi An, Xu Zhao, Tao Yu, Ming Tang, and Jinqiao Wang. Fluctuation-based adaptive structured pruning for large language models. *Proceedings of the AAAI Conference on Artificial Intelligence*, 38(10):10865–10873, Mar. 2024. doi: 10.1609/aaai.v38i10.28960. URL <https://ojs.aaai.org/index.php/AAAI/article/view/28960>.

Saleh Ashkboos, Maximilian L. Croci, Marcelo Gennari do Nascimento, Torsten Hoefer, and James Hensman. SliceGPT: Compress large language models by deleting rows and columns. In *The Twelfth International Conference on Learning Representations*, 2024. URL <https://openreview.net/forum?id=vXxardq6db>.

Jacob Austin, Augustus Odena, Maxwell Nye, Maarten Bosma, Henryk Michalewski, David Dohan, Ellen Jiang, Carrie Cai, Michael Terry, Quoc Le, and Charles Sutton. Program synthesis with large language models, 2021. URL <https://arxiv.org/abs/2108.07732>.

Abhinav Bandari, Lu Yin, Cheng-Yu Hsieh, Ajay Kumar Jaiswal, Tianlong Chen, Li Shen, Ranjay Krishna, and Shiwei Liu. Is c4 dataset optimal for pruning? an investigation of calibration data for llm pruning, 2024. URL <https://arxiv.org/abs/2410.07461>.

Tianyi Chen, Bo Ji, Tianyu Ding, Biyi Fang, Guanyi Wang, Zhihui Zhu, Luming Liang, Yixin Shi, Sheng Yi, and Xiao Tu. Only train once: A one-shot neural network training and pruning framework. In M. Ranzato, A. Beygelzimer, Y. Dauphin, P.S. Liang, and J. Wortman Vaughan, editors, *Advances in Neural Information Processing Systems*, volume 34, pages 19637–19651. Curran Associates, Inc., 2021. URL [https://proceedings.neurips.cc/paper\\_files/paper/2021/file/a376033f78e144f494bfc743c0be3330-Paper.pdf](https://proceedings.neurips.cc/paper_files/paper/2021/file/a376033f78e144f494bfc743c0be3330-Paper.pdf).

Yongchao Chen, Yilun Hao, Yueying Liu, Yang Zhang, and Chuchu Fan. Codesteer: Symbolic-augmented language models via code/text guidance. In *Forty-second International Conference on Machine Learning*.

Yongchao Chen, Yueying Liu, Junwei Zhou, Yilun Hao, Jingquan Wang, Yang Zhang, and Chuchu Fan. R1-code-interpreter: Training llms to reason with code via supervised and reinforcement learning. *arXiv preprint arXiv:2505.21668*, 2025.

Hongrong Cheng, Miao Zhang, and Javen Qinfeng Shi. A survey on deep neural network pruning: Taxonomy, comparison, analysis, and recommendations. *IEEE Transactions on Pattern Analysis and Machine Intelligence*, 46(12):10558–10578, 2024. doi: 10.1109/TPAMI.2024.3447085.

Peter Clark, Isaac Cowhey, Oren Etzioni, Tushar Khot, Ashish Sabharwal, Carissa Schoenick, and Oyvind Tafjord. Think you have solved question answering? try arc, the ai2 reasoning challenge, 2018. URL <https://arxiv.org/abs/1803.05457>.

Mingxuan Cui, Duo Zhou, Yuxuan Han, Grani A Hanusanto, Qiong Wang, Huan Zhang, and Zhengyuan Zhou. Dr-sac: Distributionally robust soft actor-critic for reinforcement learning under uncertainty. *arXiv preprint arXiv:2506.12622*, 2025.

Sizhe Dang, Yangyang Guo, Yanjun Zhao, Haishan Ye, Xiaodong Zheng, Guang Dai, and Ivor Tsang. Fzoo: Fast zeroth-order optimizer for fine-tuning large language models towards adam-scale speed, 2025. URL <https://arxiv.org/abs/2506.09034>.

Abhimanyu Dubey, Abhinav Jauhri, Abhinav Pandey, and etc. The llama 3 herd of models, 2024. URL <https://arxiv.org/abs/2407.21783>.

An Yang et al. Qwen2.5 technical report, 2025. URL <https://arxiv.org/abs/2412.15115>.

Gongfan Fang, Xinyin Ma, Mingli Song, Michael Bi Mi, and Xinchao Wang. Depgraph: Towards any structural pruning. In *Proceedings of the IEEE/CVF Conference on Computer Vision and Pattern Recognition (CVPR)*, pages 16091–16101, June 2023.

Gongfan Fang, Hongxu Yin, Saurav Muralidharan, Greg Heinrich, Jeff Pool, Jan Kautz, Pavlo Molchanov, and Xinchao Wang. MaskLLM: Learnable semi-structured sparsity for large language models. In *The Thirty-eighth Annual Conference on Neural Information Processing Systems*, 2024. URL <https://openreview.net/forum?id=Llu9nJa17b>.

Jonathan Frankle and Michael Carbin. The lottery ticket hypothesis: Finding sparse, trainable neural networks. In *International Conference on Learning Representations*, 2019. URL <https://openreview.net/forum?id=rJl-b3RcF7>.

Elias Frantar and Dan Alistarh. SparseGPT: Massive language models can be accurately pruned in one-shot. In Andreas Krause, Emma Brunskill, Kyunghyun Cho, Barbara Engelhardt, Sivan Sabato, and Jonathan Scarlett, editors, *Proceedings of the 40th International Conference on Machine Learning*, volume 202 of *Proceedings of Machine Learning Research*, pages 10323–10337. PMLR, 23–29 Jul 2023. URL <https://proceedings.mlr.press/v202/frantar23a.html>.

Elias Frantar, Saleh Ashkboos, Torsten Hoefer, and Dan Alistarh. Gptq: Accurate post-training quantization for generative pre-trained transformers, 2023.

Leo Gao, Jonathan Tow, Baber Abbasi, Stella Biderman, Sid Black, Anthony DiPofi, Charles Foster, Laurence Golding, Jeffrey Hsu, Alain Le Noac'h, Haonan Li, Kyle McDonell, Niklas Muennighoff, Chris Ociepa, Jason Phang, Laria Reynolds, Hailey Schoelkopf, Aviya Skowron, Lintang Sutawika, Eric Tang, Anish Thite, Ben Wang, Kevin Wang, and Andy Zou. The language model evaluation harness, 07 2024. URL <https://zenodo.org/records/12608602>.

Xinrui He, Yikun Ban, Jiaru Zou, Tianxin Wei, Curtiss Cook, and Jingrui He. Llm-forest: Ensemble learning of llms with graph-augmented prompts for data imputation. In *Findings of the Association for Computational Linguistics: ACL 2025*, page 6921–6936. Association for Computational Linguistics, 2025. doi: 10.18653/v1/2025.findings-acl.361. URL <http://dx.doi.org/10.18653/v1/2025.findings-acl.361>.

Edward J. Hu, Yelong Shen, Phillip Wallis, Zeyuan Allen-Zhu, Yuanzhi Li, Shean Wang, Lu Wang, and Weizhu Chen. Lora: Low-rank adaptation of large language models, 2021a. URL <https://arxiv.org/abs/2106.09685>.

Edward J. Hu, Yelong Shen, Phillip Wallis, Zeyuan Allen-Zhu, Yuanzhi Li, Shean Wang, Lu Wang, and Weizhu Chen. Lora: Low-rank adaptation of large language models, 2021b. URL <https://arxiv.org/abs/2106.09685>.

Wei Huang, Xin Zheng, Xiaoqin Ma, Haotong Qin, Cheng Lv, Haodong Chen, Jie Luo, Xiaodong Qi, and Xing Liu. An empirical study of llama3 quantization: from llms to mllms. *Visual Intelligence*, 2:36, 2024. doi: 10.1007/s44267-024-00070-x.

Leonardo Iurada, Marco Ciccone, and Tatiana Tommasi. Finding lottery tickets in vision models via data-driven spectral foresight pruning. In *Proceedings of the IEEE/CVF Conference on Computer Vision and Pattern Recognition (CVPR)*, pages 16142–16151, June 2024.

Arthur Jacot, Franck Gabriel, and Clément Hongler. Neural tangent kernel: Convergence and generalization in neural networks. *Advances in neural information processing systems*, 31, 2018.

Yixin Ji, Yang Xiang, Juntao Li, Qingrong Xia, Ping Li, Xinyu Duan, Zhefeng Wang, and Min Zhang. Beware of calibration data for pruning large language models, 2024. URL <https://arxiv.org/abs/2410.17711>.

Frederik Kunstner, Jacques Chen, Jonathan Wilder Lavington, and Mark Schmidt. Noise is not the main factor behind the gap between sgd and adam on transformers, but sign descent might be, 2023. URL <https://arxiv.org/abs/2304.13960>.

Woosuk Kwon, Sehoon Kim, Michael W Mahoney, Joseph Hassoun, Kurt Keutzer, and Amir Gholami. A fast post-training pruning framework for transformers. In S. Koyejo, S. Mohamed, A. Agarwal, D. Belgrave, K. Cho, and A. Oh, editors, *Advances in Neural Information Processing Systems*, volume 35, pages 24101–24116. Curran Associates, Inc., 2022. URL [https://proceedings.neurips.cc/paper\\_files/paper/2022/file/987bed997ab668f91c822a09bce3ea12-Paper-Conference.pdf](https://proceedings.neurips.cc/paper_files/paper/2022/file/987bed997ab668f91c822a09bce3ea12-Paper-Conference.pdf).

Yann LeCun et al. Generalization and network design strategies. *Connectionism in perspective*, 19(143-155):18, 1989.

Jaeho Lee, Sejun Park, Sangwoo Mo, Sungsoo Ahn, and Jinwoo Shin. Layer-adaptive sparsity for the magnitude-based pruning, 2021. URL <https://arxiv.org/abs/2010.07611>.

Jaehoon Lee, Lechao Xiao, Samuel Schoenholz, Yasaman Bahri, Roman Novak, Jascha Sohl-Dickstein, and Jeffrey Pennington. Wide neural networks of any depth evolve as linear models under gradient descent. In H. Wallach, H. Larochelle, A. Beygelzimer, F. d'Alché-Buc, E. Fox, and R. Garnett, editors, *Advances in Neural Information Processing Systems*, volume 32. Curran Associates, Inc., 2019a. URL [https://proceedings.neurips.cc/paper\\_files/paper/2019/file/0d1a9651497a38d8b1c3871c84528bd4-Paper.pdf](https://proceedings.neurips.cc/paper_files/paper/2019/file/0d1a9651497a38d8b1c3871c84528bd4-Paper.pdf).

Namhoon Lee, Thalaiyasingam Ajanthan, and Philip H. S. Torr. Snip: Single-shot network pruning based on connection sensitivity, 2019b. URL <https://arxiv.org/abs/1810.02340>.

Bingrui Li, Wei Huang, Andi Han, Zhanpeng Zhou, Taiji Suzuki, Jun Zhu, and Jianfei Chen. On the optimization and generalization of two-layer transformers with sign gradient descent, 2024. URL <https://arxiv.org/abs/2410.04870>.

Zihao Li, Dongqi Fu, Mengting Ai, and Jingrui He. Apex2: Adaptive and extreme summarization for personalized knowledge graphs. In *Proceedings of the 31st ACM SIGKDD Conference on Knowledge Discovery and Data Mining V.1*, KDD '25, page 741–752, New York, NY, USA, 2025. Association for Computing Machinery. ISBN 9798400712456. doi: 10.1145/3690624.3709213. URL <https://doi.org/10.1145/3690624.3709213>.

Ji Lin, Jiaming Tang, Haotian Tang, Shang Yang, Wei-Ming Chen, Wei-Chen Wang, Guangxuan Xiao, Xingyu Dang, Chuang Gan, and Song Han. Awq: Activation-aware weight quantization for on-device llm compression and acceleration. In P. Gibbons, G. Pekhimenko, and C. De Sa, editors, *Proceedings of Machine Learning and Systems*, volume 6, pages 87–100, 2024. URL [https://proceedings.mlsys.org/paper\\_files/paper/2024/file/42a452cbafa9dd64e9ba4aa95cc1ef21-Paper-Conference.pdf](https://proceedings.mlsys.org/paper_files/paper/2024/file/42a452cbafa9dd64e9ba4aa95cc1ef21-Paper-Conference.pdf).

Gui Ling, Ziyang Wang, Yuliang Yan, and Qingwen Liu. Slimgpt: Layer-wise structured pruning for large language models. In A. Globerson, L. Mackey, D. Belgrave, A. Fan, U. Paquet, J. Tomczak, and C. Zhang, editors, *Advances in Neural Information Processing Systems*, volume 37, pages 107112–107137. Curran Associates, Inc., 2024. URL [https://proceedings.neurips.cc/paper\\_files/paper/2024/file/c1c44e46358e0fb94dc94ec495a7fb1a-Paper-Conference.pdf](https://proceedings.neurips.cc/paper_files/paper/2024/file/c1c44e46358e0fb94dc94ec495a7fb1a-Paper-Conference.pdf).

Xinyin Ma, Gongfan Fang, and Xinchao Wang. Llm-pruner: On the structural pruning of large language models. In A. Oh, T. Naumann, A. Globerson, K. Saenko, M. Hardt, and S. Levine, editors, *Advances in Neural Information Processing Systems*, volume 36, pages 21702–21720. Curran Associates, Inc., 2023. URL [https://proceedings.neurips.cc/paper\\_files/paper/2023/file/44956951349095f74492a5471128a7e0-Paper-Conference.pdf](https://proceedings.neurips.cc/paper_files/paper/2023/file/44956951349095f74492a5471128a7e0-Paper-Conference.pdf).

Xin Men, Mingyu Xu, Qingyu Zhang, Bingning Wang, Hongyu Lin, Yaojie Lu, Xianpei Han, and Weipeng Chen. Shortgpt: Layers in large language models are more redundant than you expect, 2024. URL <https://arxiv.org/abs/2403.03853>.

Stephen Merity, Caiming Xiong, James Bradbury, and Richard Socher. Pointer sentinel mixture models. *arXiv preprint arXiv:1609.07843*, 2016.

Eshaan Nichani, Jason D. Lee, and Alberto Bietti. Understanding factual recall in transformers via associative memories. In *NeurIPS 2024 Workshop on Mathematics of Modern Machine Learning*, 2024. URL <https://openreview.net/forum?id=PtYojIoW0u>.

Xuying Ning, Dongqi Fu, Tianxin Wei, Wujiang Xu, and Jingrui He. Graph4mm: Weaving multi-modal learning with structural information. In *Forty-second International Conference on Machine Learning*, a.

Xuying Ning, Wujiang Xu, Tianxin Wei, and Xiaolei Liu. i2vae: Interest information augmentation with variational regularizers for cross-domain sequential recommendation. In *The 41st Conference on Uncertainty in Artificial Intelligence*, b.

NVIDIA Corporation. Train with mixed precision. <https://docs.nvidia.com/deeplearning/performance/mixed-precision-training/index.html>.

Denis Paperno, Germán Kruszewski, Angeliki Lazaridou, Ngoc Quan Pham, Raffaella Bernardi, Sandro Pezzelle, Marco Baroni, Gemma Boleda, and Raquel Fernández. The LAMBADA dataset: Word prediction requiring a broad discourse context. In Katrin Erk and Noah A. Smith, editors, *Proceedings of the 54th Annual Meeting of the Association for Computational Linguistics (Volume 1: Long Papers)*, pages 1525–1534, Berlin, Germany, August 2016. Association for Computational Linguistics. doi: 10.18653/v1/P16-1144. URL <https://aclanthology.org/P16-1144>.

Arkil Patel, Satwik Bhattacharya, and Navin Goyal. Are nlp models really able to solve simple math word problems?, 2021. URL <https://arxiv.org/abs/2103.07191>.

Colin Raffel, Noam Shazeer, Adam Roberts, Katherine Lee, Sharan Narang, Michael Matena, Yanqi Zhou, Wei Li, and Peter J. Liu. Exploring the limits of transfer learning with a unified text-to-text transformer, 2023. URL <https://arxiv.org/abs/1910.10683>.

Keisuke Sakaguchi, Ronan Le Bras, Chandra Bhagavatula, and Yejin Choi. Winogrande: An adversarial winograd schema challenge at scale. *Communications of the ACM*, 64(9):99–106, 2021.

Abdullah Salama, Oleksiy Ostapenko, Tassilo Klein, and Moin Nabi. Pruning at a glance: Global neural pruning for model compression, 2019. URL <https://arxiv.org/abs/1912.00200>.

Valerie Sarge, Michael Andersch, Lynsey Fabel, Paulius Micikevicius, and John Tran. Tips for optimizing gpu performance using tensor cores. <https://developer.nvidia.com/blog/optimizing-gpu-performance-tensor-cores/>, June 2019.

Noam Shazeer. Glu variants improve transformer, 2020. URL <https://arxiv.org/abs/2002.05202>.

Mingjie Sun, Zhuang Liu, Anna Bair, and J. Zico Kolter. A simple and effective pruning approach for large language models. *arXiv preprint arXiv:2306.11695*, 2023.

Hidekori Tanaka, Daniel Kunin, Daniel L Yamins, and Surya Ganguli. Pruning neural networks without any data by iteratively conserving synaptic flow. In H. Larochelle, M. Ranzato, R. Hadsell, M.F. Balcan, and H. Lin, editors, *Advances in Neural Information Processing Systems*, volume 33, pages 6377–6389. Curran Associates, Inc., 2020. URL [https://proceedings.neurips.cc/paper\\_files/paper/2020/file/46a4378f835dc8040c8057beb6a2da52-Paper.pdf](https://proceedings.neurips.cc/paper_files/paper/2020/file/46a4378f835dc8040c8057beb6a2da52-Paper.pdf).

Rohan Taori, Ishaan Gulrajani, Tianyi Zhang, Yann Dubois, Xuechen Li, Carlos Guestrin, Percy Liang, and Tatsunori B. Hashimoto. Stanford alpaca: An instruction-following llama model. [https://github.com/tatsu-lab/stanford\\_alpaca](https://github.com/tatsu-lab/stanford_alpaca), 2023.

Yijun Tian, Yikun Han, Xiusi Chen, Wei Wang, and Nitesh V. Chawla. Beyond answers: Transferring reasoning capabilities to smaller llms using multi-teacher knowledge distillation. In *Proceedings of the Eighteenth ACM International Conference on Web Search and Data Mining, WSDM '25*, page 251–260, New York, NY, USA, 2025. Association for Computing Machinery. ISBN 9798400713293. doi: 10.1145/3701551.3703577. URL <https://doi.org/10.1145/3701551.3703577>.

Ashish Vaswani, Noam Shazeer, Niki Parmar, Jakob Uszkoreit, Llion Jones, Aidan N Gomez, Łukasz Kaiser, and Illia Polosukhin. Attention is all you need. *Advances in neural information processing systems*, 30, 2017.

Artem Vysogorets and Julia Kempe. Connectivity matters: Neural network pruning through the lens of effective sparsity. *Journal of Machine Learning Research*, 24(99):1–23, 2023. URL <http://jmlr.org/papers/v24/22-0415.html>.

Patrick Wagner, Nils Strothoff, Ralf-Dieter Bousseljot, Dieter Kreiseler, Fatima I Lunze, Wojciech Samek, and Tobias Schaeffer. PtB-XL, a large publicly available electrocardiography dataset. *Scientific data*, 7(1):1–15, 2020.

Bo Yao Wang, Rui Pan, Shizhe Diao, Xingyuan Pan, Jipeng Zhang, Renjie Pi, and Tong Zhang. Adapt-pruner: Adaptive structural pruning for efficient small language model training, 2025. URL <https://arxiv.org/abs/2502.03460>.

Chaoqi Wang, Guodong Zhang, and Roger Grosse. Picking winning tickets before training by preserving gradient flow, 2020. URL <https://arxiv.org/abs/2002.07376>.

Yite Wang, Dawei Li, and Ruoyu Sun. Ntk-sap: Improving neural network pruning by aligning training dynamics, 2023. URL <https://arxiv.org/abs/2304.02840>.

Tianxin Wei, Zeming Guo, Yifan Chen, and Jingrui He. NTK-approximating MLP fusion for efficient language model fine-tuning. In Andreas Krause, Emma Brunskill, Kyunghyun Cho, Barbara Engelhardt, Sivan Sabato, and Jonathan Scarlett, editors, *Proceedings of the 40th International Conference on Machine Learning*, volume 202 of *Proceedings of Machine Learning Research*, pages 36821–36838. PMLR, 23–29 Jul 2023. URL <https://proceedings.mlr.press/v202/wei23b.html>.

Miles Williams and Nikolaos Aletras. On the impact of calibration data in post-training quantization and pruning. In *Proceedings of the 62nd Annual Meeting of the Association for Computational Linguistics (Volume 1: Long Papers)*, page 10100–10118. Association for Computational Linguistics, 2024. doi: 10.18653/v1/2024.acl-long.544. URL <http://dx.doi.org/10.18653/v1/2024.acl-long.544>.

Mengzhou Xia, Tianyu Gao, Zhiyuan Zeng, and Danqi Chen. Sheared llama: Accelerating language model pre-training via structured pruning, 2024. URL <https://arxiv.org/abs/2310.06694>.

Guangxuan Xiao, Ji Lin, Mickael Seznec, Hao Wu, Julien Demouth, and Song Han. SmoothQuant: Accurate and efficient post-training quantization for large language models. In Andreas Krause, Emma Brunskill, Kyunghyun Cho, Barbara Engelhardt, Sivan Sabato, and Jonathan Scarlett, editors, *Proceedings of the 40th International Conference on Machine Learning*, volume 202 of *Proceedings of Machine Learning Research*, pages 38087–38099. PMLR, 23–29 Jul 2023. URL <https://proceedings.mlr.press/v202/xiao23c.html>.

Huanrui Yang, Hongxu Yin, Maying Shen, Pavlo Molchanov, Hai Li, and Jan Kautz. Global vision transformer pruning with hessian-aware saliency. In *Proceedings of the IEEE/CVF Conference on Computer Vision and Pattern Recognition (CVPR)*, pages 18547–18557, June 2023.

Rowan Zellers, Ari Holtzman, Yonatan Bisk, Ali Farhadi, and Yejin Choi. Hellaswag: Can a machine really finish your sentence?, 2019. URL <https://arxiv.org/abs/1905.07830>.

Yuji Zhang, Jing Li, and Wenjie Li. VIBE: Topic-driven temporal adaptation for Twitter classification. In Houda Bouamor, Juan Pino, and Kalika Bali, editors, *Proceedings of the 2023 Conference on Empirical Methods in Natural Language Processing*, pages 3340–3354, Singapore, December 2023. Association for Computational Linguistics. doi: 10.18653/v1/2023.emnlp-main.203. URL <https://aclanthology.org/2023.emnlp-main.203/>.

Yuji Zhang, Sha Li, Jiateng Liu, Pengfei Yu, Yi R Fung, Jing Li, Manling Li, and Heng Ji. Knowledge overshadowing causes amalgamated hallucination in large language models. *arXiv preprint arXiv:2407.08039*, 2024.

Kai Zhao, Yanjun Zhao, Jiaming Song, Shien He, Lusheng Zhang, Qiang Zhang, and Tianjiao Li. Saber: Switchable and balanced training for efficient llm reasoning, 2025a. URL <https://arxiv.org/abs/2508.10026>.

Yanjun Zhao, Ziqing Ma, Tian Zhou, Mengni Ye, Liang Sun, and Yi Qian. Gcformer: An efficient solution for accurate and scalable long-term multivariate time series forecasting. In *Proceedings of the 32nd ACM International Conference on Information and Knowledge Management*, CIKM '23, page 3464–3473, New York, NY, USA, 2023. Association for Computing Machinery. ISBN 9798400701245. doi: 10.1145/3583780.3615136. URL <https://doi.org/10.1145/3583780.3615136>.

Yanjun Zhao, Tian Zhou, Chao Chen, Liang Sun, Yi Qian, and Rong Jin. Sparse-vq transformer: An ffn-free framework with vector quantization for enhanced time series forecasting, 2024. URL <https://arxiv.org/abs/2402.05830>.

Yanjun Zhao, Sizhe Dang, Haishan Ye, Guang Dai, Yi Qian, and Ivor W. Tsang. Second-order fine-tuning without pain for llms:a hessian informed zeroth-order optimizer, 2025b. URL <https://arxiv.org/abs/2402.15173>.

Haizhong Zheng, Xiaoyan Bai, Xueshen Liu, Z. Morley Mao, Beidi Chen, Fan Lai, and Atul Prakash. Learn to be efficient: Build structured sparsity in large language models, 2024. URL <https://arxiv.org/abs/2402.06126>.

Difan Zou, Yuan Cao, Yuanzhi Li, and Quanquan Gu. Understanding the generalization of adam in learning neural networks with proper regularization, 2021. URL <https://arxiv.org/abs/2108.11371>.

Jiaru Zou, Mengyu Zhou, Tao Li, Shi Han, and Dongmei Zhang. Promptintern: Saving inference costs by internalizing recurrent prompt during large language model fine-tuning, 2024. URL <https://arxiv.org/abs/2407.02211>.

Jiaru Zou, Yikun Ban, Zihao Li, Yunzhe Qi, Ruizhong Qiu, Ling Yang, and Jingrui He. Transformer copilot: Learning from the mistake log in llm fine-tuning, 2025a. URL <https://arxiv.org/abs/2505.16270>.

Jiaru Zou, Dongqi Fu, Sirui Chen, Xinrui He, Zihao Li, Yada Zhu, Jiawei Han, and Jingrui He. Gtr: Graph-table-rag for cross-table question answering. *arXiv preprint arXiv:2504.01346*, 2025b.

Jiaru Zou, Ling Yang, Jingwen Gu, Jiahao Qiu, Ke Shen, Jingrui He, and Mengdi Wang. Reasonflux-prm: Trajectory-aware prms for long chain-of-thought reasoning in llms, 2025c. URL <https://arxiv.org/abs/2506.18896>.

## A RELATED WORK

While Section 2 and Section 3.2 provide a high-level overview of LLM structured pruning, this appendix offers a more comprehensive discussion. The landscape of modern AI is fundamentally shaped by the Transformer architecture (Zou et al., 2025b; Chen et al.; Zhang et al., 2024; 2023; Cui et al., 2025), whose scaling capabilities have driven unprecedented progress across different tasks (Zou et al., 2025a;c; Chen et al., 2025; He et al., 2025; Ning et al., b;a). This success, however, has also necessitated a strong focus on computational efficiency to manage the growing resource demands of large models (Zhao et al., 2023; 2025b;a; Li et al., 2025). Against this backdrop, we now dive into a more detailed analysis of existing pruning methodologies.

### A.1 NOTATIONS

We use lowercase letters to denote scalars, boldface lowercase letters for vectors, and boldface uppercase letters for matrices. The element-wise product is denoted by  $\odot$ . Let  $f(\mathbf{x}; \mathbf{W} \odot \mathbf{M})$  denote the neural network function, where  $\mathbf{x}$  are the inputs,  $\mathbf{W}$  the weights (or connections), and  $\mathbf{M}$  the sparse mask matrix with sparsity  $v$  (density  $d = 1 - v$ ). Additionally, let  $\mathcal{L}$  be the loss function, and let

$$D = \{(\mathbf{x}_k, \mathbf{y}_k)\}_{k=1}^N \subset \mathbb{R}^n \times \mathbb{R}^m$$

denote the dataset with  $N$  data points (with  $\mathbf{x}$  as the input features and  $\mathbf{y}$  as the labels). Finally, let  $\mathcal{A}$  be the optimizer that, given the initial weights of the network before supervised fine-tuning (SFT)  $\mathbf{W}^{(0)}$ , returns the weights after SFT, i.e.,  $\mathbf{W}^{(\text{final})} = \mathcal{A}(\mathbf{W}^{(0)})$ . See the full notation in Table 4.

### A.2 POST-TRAIN PRUNING

Post-train pruning compresses a fully trained dense model by removing unimportant weights or structures. A common formulation minimizes the discrepancy between the outputs of the uncompressed and pruned layers. Given an input  $\mathbf{x}$ , the objective is to solve:

$$\begin{aligned} & \operatorname{argmin}_{\hat{\mathbf{W}}, \mathbf{M}} \mathcal{L}(\mathbf{W}^{(\text{final})} \mathbf{x}, (\hat{\mathbf{W}} \odot \mathbf{M}) \mathbf{x}) \\ &= \operatorname{argmin}_{\hat{\mathbf{W}}, \mathbf{M}} \frac{1}{N} \sum_{k=1}^N \mathcal{L}(\mathbf{W}^{(\text{final})} \mathbf{x}_k, (\hat{\mathbf{W}} \odot \mathbf{M}) \mathbf{x}_k), \end{aligned}$$

where  $\mathbf{M}$  is a mask matrix enforcing a fixed sparsity  $v$ .

Directly solving this joint optimization over  $\hat{\mathbf{W}}$  and  $\mathbf{M}$  is NP-hard. Consequently, popular practices include fixing the weights (i.e., setting  $\hat{\mathbf{W}} = \mathbf{W}$ ) and searching for  $\mathbf{M}$  only (one-shot pruning (Frankle and Carbin, 2019; Frantar and Alistarh, 2023; Sun et al., 2023; Chen et al., 2021)), or selecting  $\mathbf{M}$  first and then optimizing  $\hat{\mathbf{W}}$  (which typically requires further fine-tuning or re-training (Kwon et al., 2022; Ma et al., 2023)).

### A.3 FORESIGHT PRUNING

Foresight pruning, also known as pruning before training, seeks to identify and eliminate redundant parameters at initialization, thereby reducing both training and inference costs. For a neural network  $f$  parameterized by  $\mathbf{W}$  and data  $(\mathbf{x}, \mathbf{y})$ , the objective is formulated as:

$$\begin{aligned} & \min_{\mathbf{M}} \mathcal{L}(f(\mathbf{x}; \mathcal{A}(\mathbf{W}^{(0)} \odot \mathbf{M})), \mathbf{y}) \\ &= \min_{\mathbf{M}} \frac{1}{N} \sum_{k=1}^N \mathcal{L}(f(\mathbf{x}_k; \mathcal{A}(\mathbf{W}^{(0)} \odot \mathbf{M})), \mathbf{y}_k), \end{aligned} \tag{5}$$

where  $\mathcal{A}$  returns the final weights  $\mathbf{W}^{(\text{final})}$ . As in the post-train case, solving Equation (5) exactly is NP-hard because it involves joint optimization over the mask and the model parameters.

Table 4: Notation.

Symbol	Definition and Description
$\mathbf{x}$	Input token, $\mathbf{x} \in \mathbb{R}^d$
$f(\mathbf{x}; \mathbf{W} \odot \mathbf{M})$	Neural network function, with weights $\mathbf{W}$ and sparse mask $\mathbf{M}$
$\mathbf{W}$	Weight matrices (parameters) of the network
$\mathbf{M}$	Binary mask matrix, $\mathbf{M} \in \{0, 1\}^{\text{shape}(\mathbf{W})}$ , indicating pruned weights
$\mathcal{D}$	Dataset
$S$	Saliency score function
$\odot$	Element-wise (Hadamard) product
$\sigma(\cdot)$	Swish activation function, applied elementwise
$v$	Sparsity ratio
$d$	Hidden size of the model
$m$	Intermediate (FFN) dimension in the MLP
$h$	Number of attention heads
$d_h$	Per-head dimension, $d_h = d/h$
$\mathbf{W}_a^Q, \mathbf{W}_a^K, \mathbf{W}_a^V$	Query, Key, Value weight matrices for head $i$ , each $\in \mathbb{R}^{d \times d_h}$
$\mathbf{W}_a^O$	Output weight matrices for head $i$ , $\in \mathbb{R}^{d_h \times d}$
$\mathbf{Q}_a, \mathbf{K}_a, \mathbf{V}_a$	Query, Key, Value representations for head $i$
$\mathbf{W}_{\text{gate}}, \mathbf{W}_{\text{up}}$	Projection weights, $\in \mathbb{R}^{d \times m}$
$\mathbf{W}_{\text{down}}$	Down projection weight, $\in \mathbb{R}^{m \times d}$
$\text{head}_a$	Attention output for head $a$
$\text{MHA}(\mathbf{x})$	Multi-Head Attention output
$\mathbf{H}(\mathbf{x})$	MLP block output

To bridge this gap, popular approaches define a *saliency score*  $S_{i,j}$  for each weight, which estimates the impact of removing the connection  $\mathbf{W}_{i,j}$ . A general form of the saliency score is:

$$S(\mathbf{W}_{i,j}^{(0)}) = \frac{\partial \mathcal{I}}{\partial \mathbf{W}_{i,j}^{(0)}} \cdot \mathbf{W}_{i,j}^{(0)}, \quad (6)$$

where  $\mathcal{I}$  is a function that measures the importance of the weight  $\mathbf{W}$  to the network  $f$ . Once these scores are computed, the mask is obtained by selecting the top  $\kappa\%$  of weights:

$$\mathbf{M}_{i,j} = \text{Top}_\kappa(S)_{i,j} = \begin{cases} 1, & \text{if } S_{i,j} \text{ is among the top } \kappa\%, \\ 0, & \text{otherwise.} \end{cases}$$

#### A.4 REVISITING SALIENCY METHODS

Several representative methods use different formulations of the saliency score to approximate weight importance. These approaches are predominantly explored in the context of computer vision tasks. In the following sections, we will also discuss the work in the LLM context.

**SNIP** (Lee et al., 2019b) proposes a data-dependent saliency:

$$S_{\text{SNIP}} = \left| \frac{\partial \mathcal{L}(\mathbf{x}; \mathbf{W})}{\partial \mathbf{W}_{i,j}} \cdot \mathbf{W}_{i,j} \right|.$$

**GraSP** (Wang et al., 2020) employs a second-order (Hessian) metric:

$$S_{\text{GraSP}} = - \left( \mathbf{H} \frac{\partial \mathcal{L}(\mathbf{x}; \mathbf{W})}{\partial \mathbf{W}_{i,j}} \right) \cdot \mathbf{W}_{i,j},$$

where  $\mathbf{H}$  denotes the Hessian of the loss.

**SynFlow** (Tanaka et al., 2020) introduces a data-agnostic approach by defining saliency on constant inputs (e.g.,  $\mathbf{1}$ ) and absolute weights:

$$S_{\text{SynFlow}} = \left| \frac{\partial f(\mathbf{1}; |\mathbf{W}|)}{\partial |\mathbf{W}_{i,j}|} \right| \cdot |\mathbf{W}_{i,j}|.$$

Although SynFlow’s formulation is similar to our approach, using absolute values may not fully capture the true gradient flow in the model.

**NTK-SAP** (Wang et al., 2023) adopts a data-agnostic perspective by injecting a small perturbation  $\Delta \mathbf{W}_{i,j} \sim \mathcal{N}(0, \epsilon \mathbf{I})$ :

$$S_{\text{NTK-SAP}} = \left| \frac{\partial \|f(\mathbf{z}; \mathbf{W}) - f(\mathbf{z}; \mathbf{W} + \Delta \mathbf{W})\|_2^2}{\partial \mathbf{W}_{i,j}} \right|,$$

with  $\mathbf{z}$  drawn from a standard normal distribution.

**PX-Pruning** (Iurada et al., 2024) introduces an auxiliary function  $\mathcal{R}$  computed by two helper networks  $g$  and  $h$  (sharing the original architecture):

$$S_{\text{PX}} = \left| \frac{\partial \mathcal{R}(\mathbf{x}, \mathbf{W}, \mathbf{a})}{\partial (\mathbf{W}_{i,j}^2)} \cdot \mathbf{W}_{i,j}^2 \right|,$$

where

$$\mathcal{R}(\mathbf{x}, \mathbf{W}, \mathbf{a}) = g(\mathbf{x}^2, \mathbf{1}, \mathbf{a}) h(\mathbf{1}, \mathbf{W}^2, \mathbf{1}),$$

and  $\mathbf{a}$  tracks the activation status. Backpropagation through  $\mathcal{R}$  yields a saliency score for each parameter.

While these foresight methods have shown promise, they are not commonly applied to LLMs due to the models’ scale and behavior during fine-tuning. Moreover, the inherent nature of unstructured pruning in these methods often limits their ability to reduce training costs. In contrast, our work focuses on the MLP module in LLMs and develops an NTK-aware saliency score tailored to preserve training dynamics.

### A.5 LLM-BASED PRUNING

Recent unstructured pruning methods, such as SparseGPT (Frantar and Alistarh, 2023) and Wanda (Sun et al., 2023), have proposed efficient one-shot pruning strategies that remove individual weights based on local reconstruction error or activation-aware criteria. While effective in preserving accuracy, their irregular sparsity patterns limit practical speedups on existing hardware accelerators.

In contrast, structured pruning methods aim to remove entire neurons, attention heads, or layers, enabling more hardware-friendly sparsity. Representative approaches include LLM-Pruner (Ma et al., 2023), Sheared Llama (Xia et al., 2024), and SlimGPT (Ling et al., 2024), which prune model components based on local importance scores. However, these methods typically ignore the underlying optimization dynamics and treat attention and MLP modules uniformly, potentially leading to sub-optimal performance.

Several recent works have attempted to address the imbalance across layers. For example, Adapt-Pruner (Wang et al., 2025) introduces layer-wise global scoring but still applies uniform pruning within modules, neglecting the distinct pruning characteristics between attention and MLP. FLAP (An et al., 2024) further introduces a heuristic structure search to assign different sparsity levels across both layers and modules. However, its approach relies on standardizing fluctuation metrics without explicitly modeling the functional differences between components. Similarly, ShortGPT (Men et al., 2024) removes entire layers based on global layer importance, but does not differentiate between module types within layers.

SliceGPT (Ashkboos et al., 2024) instead prunes hidden dimensions rather than intermediate MLP or attention dimensions, leveraging computational invariance in RMSNorm-connected transformers, applying PCA-based transformations per block to identify and prune less informative components. The heavy reliance on calibration data to compute these transformations makes it sensitive to the choice of calibration dataset. More broadly, we observe that most existing methods overlook the influence of calibration data on pruning decisions, despite its critical role in ensuring stable and generalizable pruning outcomes across tasks.

In summary, while recent methods have started exploring global or layer-wise pruning strategies, they still largely neglect the distinct pruning dynamics and roles of attention heads versus MLP neurons, as well as the interplay with calibration data selection. Our work addresses these gaps

through a theoretically grounded approach that jointly considers optimization dynamics, adaptive sparsity allocation, and calibration-aware pruning.

#### A.6 NEURAL TANGENT KERNEL (NTK)

**SGD Perspective.** Consider training via continuous-time gradient descent (GD) with learning rate  $\eta$ , where the parameter vector  $\mathbf{W}_t$  evolves over time  $t$ . For a neural network  $f(\mathbf{x}; \mathbf{W})$  with training loss  $\mathcal{L}$ , one can write (Lee et al., 2019a):

$$\begin{aligned}\dot{\mathbf{W}}_t &= -\eta \nabla_{\mathbf{W}_t} f(\mathbf{x}; \mathbf{W}_t)^\top \nabla_{f(\mathbf{x}; \mathbf{W}_t)} \mathcal{L}, \\ \dot{\mathcal{L}} &= \nabla_{f(\mathbf{x}; \mathbf{W}_t)} \mathcal{L}^\top \nabla_{\mathbf{W}_t} f(\mathbf{x}; \mathbf{W}_t) \dot{\mathbf{W}}_t \\ &= -\eta \nabla_f \mathcal{L}^\top \left[ \nabla_{\mathbf{W}} f(\mathbf{x}; \mathbf{W}_t) \nabla_{\mathbf{W}} f(\mathbf{x}; \mathbf{W}_t)^\top \right] \nabla_f \mathcal{L}.\end{aligned}$$

The factor  $\nabla_{\mathbf{W}} f(\mathbf{x}; \mathbf{W}_t) \nabla_{\mathbf{W}} f(\mathbf{x}; \mathbf{W}_t)^\top$  is called the *Neural Tangent Kernel (NTK)* (Jacot et al., 2018) under SGD, denoted

$$\hat{\Theta}^{\text{SGD}}(\mathbf{x}, \mathbf{x}) = \nabla_{\mathbf{W}} f(\mathbf{x}; \mathbf{W}) \nabla_{\mathbf{W}} f(\mathbf{x}; \mathbf{W})^\top = \langle \nabla_{\mathbf{W}} f(\mathbf{x}; \mathbf{W}), \nabla_{\mathbf{W}} f(\mathbf{x}; \mathbf{W}) \rangle.$$

**Adam (SignGD) Perspective.** Modern Transformer-based language models commonly use *Adam* rather than plain SGD. Considering Adam’s exact analysis is more complicated, existing work (Li et al., 2024; Zou et al., 2021; Kunstner et al., 2023; Wei et al., 2023) suggests that *Sign Gradient Descent* (SignGD) often behaves similarly in training dynamics. Hence, as a proxy for Adam, we consider a *sign-based* update:

$$\dot{\mathbf{W}}_t = -\eta \text{sign} \left( \nabla_{\mathbf{W}} f(\mathbf{x}; \mathbf{W}_t)^\top \nabla_{f(\mathbf{x}; \mathbf{W}_t)} \mathcal{L} \right).$$

By the chain rule,

$$\begin{aligned}\dot{\mathcal{L}} &= \nabla_{f(\mathbf{x}; \mathbf{W}_t)} \mathcal{L}^\top \nabla_{\mathbf{W}} f(\mathbf{x}; \mathbf{W}_t) \dot{\mathbf{W}}_t \\ &= -\eta \nabla_f \mathcal{L}^\top \left[ \nabla_{\mathbf{W}} f(\mathbf{x}; \mathbf{W}_t) \text{sign}(\nabla_{\mathbf{W}} f(\mathbf{x}; \mathbf{W}_t))^\top \right] \nabla_f \mathcal{L}.\end{aligned}$$

Following the NTK viewpoint, we define the *asymmetric SignGD kernel* as

$$\hat{\Theta}^{\text{A-Sign}}(\mathbf{x}, \mathbf{x}) = \nabla_{\mathbf{W}} f(\mathbf{x}; \mathbf{W}) \text{sign}(\nabla_{\mathbf{W}} f(\mathbf{x}; \mathbf{W}))^\top = \langle \nabla_{\mathbf{W}} f(\mathbf{x}; \mathbf{W}), \text{sign}(\nabla_{\mathbf{W}} f(\mathbf{x}; \mathbf{W})) \rangle.$$

For simplicity, we write  $\Theta = \hat{\Theta}^{\text{A-Sign}}$  in what follows.

## B ADDITIONAL RESULTS

### B.1 ADDITIONAL ON LLAMA-3.2-3B

As shown in Table 5, similar to the main experiment in Table 1, our method consistently achieves the best performance across all sparsity levels and evaluation tasks, particularly demonstrating strong robustness in both perplexity and downstream zero-shot tasks. Compared to LLM-Pruner and SliceGPT, our method yields significantly lower perplexity and higher task accuracy under the same compression ratio, highlighting its effectiveness in preserving both language modeling capacity and generalization abilities after pruning.

### B.2 ZERO-SHOT ON QWEN2.5-7B

Table 6 shows the evaluation results on Qwen2.5-7B. Across different sparsity levels, our method consistently achieves the best overall performance. Notably, at the extreme sparsity level of 50%, LLM-Pruner encounters severe degradation and unstable outputs, while our approach still maintains reasonable perplexity and accuracy, demonstrating stronger robustness under high compression ratios.

Table 5: Evaluation results of Llama3.2-3B. **Bold** indicates the best results while underline indicates the second-best.

Sparsity	Method	WikiT ↓	PTB ↓	LambD ↓	ARC-e	WinoG	HellaS	MBPP*	#Param
0%	Llama3.2-3B	10.42	16.91	22.76	74.54	69.38	73.55	38.00	3.21B
20%	LLM-Pruner	24.61	<u>58.12</u>	<u>37.52</u>	<b>59.81</b>	<u>58.25</u>	<u>54.55</u>	<u>3.60</u>	2.70B
	SliceGPT	<u>23.85</u>	144.41	220.20	46.59	57.85	44.06	0.00	3.31B
	NIRVANA	<b>17.73</b>	<b>26.20</b>	<b>33.12</b>	59.64	<b>59.35</b>	<b>55.40</b>	<b>16.40</b>	2.65B
40%	LLM-Pruner	87.25	<u>148.41</u>	<u>90.02</u>	<u>37.04</u>	50.67	<u>31.64</u>	0.00	2.10B
	SliceGPT	<u>54.28</u>	460.73	482.84	33.80	<u>51.07</u>	30.71	0.00	2.52B
	NIRVANA (ours)	<b>43.87</b>	<b>59.96</b>	<b>65.86</b>	<b>41.08</b>	<b>52.96</b>	<b>37.89</b>	<b>0.4</b>	2.09B
50%	LLM-Pruner	252.46	<u>367.33</u>	<u>179.02</u>	29.17	49.17	26.70	0.00	1.80B
	SliceGPT	<u>83.25</u>	670.36	691.64	<u>29.63</u>	<b>50.83</b>	<u>28.72</u>	0.00	2.15B
	NIRVANA (ours)	<b>79.44</b>	<b>108.58</b>	<b>119.25</b>	<b>34.68</b>	<u>50.59</u>	<b>33.46</b>	0.00	1.81B

\*Pass@1. 3-shot.

Table 6: Evaluation results of Qwen2.5-7B. **Bold** indicates the best results.

Sparsity	Method	WikiT ↓	PTB ↓	LambD ↓	ARC-e	WinoG	HellaS	MBPP*	#Param
0%	Qwen2.5-7B	9.05	15.64	22.41	80.47	72.85	78.86	64.20	7.62B
20%	LLM-Pruner	17.73	33.12	34.17	60.44	54.93	60.30	12.4	6.27B
	NIRVANA (ours)	17.73	<b>29.22</b>	<b>32.10</b>	<b>68.98</b>	<b>65.69</b>	<b>69.24</b>	<b>32.6</b>	6.31B
40%	LLM-Pruner	<b>33.64</b>	<b>63.83</b>	<b>48.18</b>	43.69	53.91	42.98	0.0	5.13B
	NIRVANA (ours)	37.52	72.33	48.94	<b>51.26</b>	<b>58.33</b>	<b>54.22</b>	<b>5.0</b>	5.19B
50%	LLM-Pruner	8625.69	11789.92	8625.69	24.79	51.38	25.73	0.00	4.35B
	NIRVANA (ours)	<b>77.00</b>	<b>148.41</b>	<b>79.44</b>	<b>38.43</b>	<b>52.80</b>	<b>38.50</b>	0.00	4.34B

\*Pass@1. 3-shot.

### B.3 FINE-TUNING ON T5

Due to the high computational cost of fine-tuning and our observation that attention heads retain more critical information than MLP neurons, we conduct experiments on T5-base (Raffel et al., 2023) by pruning only the MLP layers, while keeping the attention heads intact. All MLP layers are pruned to a global sparsity of 50%.

We compare our method with several baselines, including classic unstructured foresight pruning methods originally proposed for vision models—SNIP (Lee et al., 2019b), SynFlow (Tanaka et al., 2020), and NTK-SAP (Wang et al., 2023)—as well as LLM-specific pruning methods such as Wanda (Sun et al., 2023) and LLM-Pruner (Ma et al., 2023). For foresight baselines, we adapt their saliency criteria within our framework to ensure a fair comparison, while for Wanda and LLM-Pruner we directly follow their official implementations, using the parameter-second variant for LLM-Pruner.

We note that the comparison here focuses exclusively on the fine-tuning setting. This is because structured pruning methods without recovery typically suffer from significant zero-shot degradation, making direct comparison with unstructured methods—which often retain better zero-shot performance—unfair. However, after sufficient supervised fine-tuning (SFT), the performance gap between structured and unstructured methods narrows considerably, allowing for a more meaningful comparison under the fine-tuning scenario. All experiments are conducted on a single V100-SXM2-32GB GPU.

Table 7 presents the fine-tuning performance of NIRVANA and baseline methods on selected GLUE tasks. We observe the following: (1) NIRVANA consistently outperforms the baseline methods. This empirically proves our theory that using NTK-based pruning criteria leads to better preservation of the model’s learning dynamics compared to other baselines. This is especially impressive since NIRVANA is on par and even manages to surpass the performance of those unstructured pruning methods such as Wanda and SNIP. (2) While SynFlow considers gradients with respect to the model’s output, its reliance on synthetic inputs leads to suboptimal results. Similarly, NTK-SAP approximates

Table 7: Evaluation results (accuracy) of t5-base on GLUE datasets. **Bold** indicates the best results while underline indicates the second-best.

	MRPC	CoLA	SST2	MNLI
t5-base	91.42	83.89	94.84	86.27
Magnitude	84.80	71.81	92.43	83.74
SNIP	<u>90.20</u>	<u>82.17</u>	<b>94.50</b>	<u>85.86</u>
SynFlow	85.29	78.04	90.94	80.97
NTK-SAP	88.24	81.30	93.35	85.16
Wanda	<b>90.69</b>	<u>82.17</u>	93.81	85.67
LLM-Pruner	<u>90.20</u>	81.20	93.58	85.37
NIRVANA (ours)	<b>90.69</b>	<b>82.45</b>	<u>94.27</u>	<b>85.99</b>

Table 8: Post-pruning statistics during inference, tested on 20 rounds of Wikitext (batch size 32).

Model	#Params	FLOPs (G)	Latency (s/batch) ↓	Throughput (tokens/s) ↑	Peak Memory (GB)
Llama-3.1-8B	8.03	6.98	0.34	12047.06	17.95
Uniform-11468	6.73	5.75	0.45	9102.22	15.46
Uniform-11472	6.73	5.75	0.33	12412.12	15.46
Layer-wise	6.73	5.75	0.33	12412.12	15.45
Attention-only	6.73	6.15	0.29	14124.14	14.70
MLP-only	6.73	5.68	0.28	14628.57	15.54

NTK using first-order Taylor expansion in a weight-agnostic way, weakening the performance under the pre-trained language model scenario.

#### B.4 EFFICIENCY ANALYSIS

We provide the inference efficiency analysis on Llama3.1-8B in Section 5.4. Here, we provide additional experiments on T5 about the fine-tuning efficiency. We also provide experiments to support our conclusion that ensuring a dimension of multiples of 8 is critical to the model’s latency and throughput.

**Fine-tuning Efficiency.** Table 9 shows the impact of pruning on computational cost on a single V100. NIRVANA reduces memory usage by 19.2% and achieves a 1.3× speedup in fine-tuning, demonstrating its practical advantage over dense models. In contrast, although SNIP utilizes a similar saliency score, it applies unstructured pruning, which is not easily exploitable by standard hardware or deep learning libraries for runtime acceleration. As a result, SNIP’s fine-tuning time and memory usage remain nearly identical to the dense model.

**Sanity-check Experiments on Dimension.** To validate our conclusion in Section 5.4, we focused on the MLP component (attention heads are pruned in groups and remain multiples of 8) with the same sparsity level. Specifically, we evaluated:

- Uniform-11468: MLP intermediate =11,468 (not divisible by 8)
- Uniform-11472: MLP intermediate =11,472 (divisible by 8)
- Layer-wise: MLP dims vary per layer (divisible by 8)

We also isolated pruning effects on each subcomponent by creating:

- Attention-only: pruning concentrated on attention heads (retaining only one head, adjusting MLP to match total params)
- MLP-only: pruning concentrated on the MLP layers (only prune MLPs)

Table 10: Performance of Llama3.1-8B with NIRVANA and SmoothQuant INT8 quantization. Lower perplexity (PPL) is better ( $\downarrow$ ). Higher throughput is better ( $\uparrow$ ).

Method	WikiT $\downarrow$	PTB $\downarrow$	LambD $\downarrow$	Latency (s/batch) $\downarrow$	Throughput (tok/s) $\uparrow$	Peak Memory (GB) $\downarrow$
Llama3.1-8B (Base)	8.50	14.02	20.09	0.35	11702.86	17.95
Llama3.1-8B.int8	8.64	14.24	20.40	0.44	9309.09	11.50
NIRVANA-0.2	13.38	19.77	26.20	0.49	8359.18	15.29
NIRVANA-0.2.int8	13.59	20.09	26.60	1.15	3561.74	10.15
NIRVANA-0.4	28.33	38.72	43.19	0.40	10240.00	12.65
NIRVANA-0.4.int8	28.77	39.33	43.87	0.96	4266.67	8.79
NIRVANA-0.5	48.94	70.11	70.11	0.36	11377.78	11.27
NIRVANA-0.5.int8	49.71	70.11	70.11	0.75	5461.33	8.08

These studies in Table 8 yield several key insights into the practical efficiency of structured pruning. First, the specific distribution of sparsity—whether applied uniformly across layers or on a layer-wise basis—exerts a negligible influence on inference latency. More critically, our results reveal that hardware-aware dimension alignment profoundly impacts runtime performance. For example, the Uniform-11468 model, with dimensions not divisible by 8, incurs a substantial latency penalty compared to its aligned Uniform-11472 counterpart, despite both models possessing an identical theoretical computational cost (FLOPs). Furthermore, we observe a trade-off based on the pruning target: applying sparsity to MLP layers yields more significant latency reductions, while pruning attention components results in a more pronounced decrease in the memory footprint. Collectively, these findings underscore the principle that dimension regularization is essential for translating theoretical FLOP reductions into tangible inference acceleration. This insight provides a clear directive for developing pruning methods that are not only accurate but also optimized for efficient, real-world deployment on modern hardware.

## C SYNERGY WITH QUANTIZATION

This section explores the relationship between our structured pruning method, NIRVANA, and quantization (Xiao et al., 2023; Lin et al., 2024; Frantar et al., 2023), another prominent model compression technique. We demonstrate that they are *orthogonal* and can be combined for compounded efficiency gains.

### C.1 PRUNING VS. QUANTIZATION

Structured pruning and quantization enhance model efficiency through distinct mechanisms:

Structured Pruning modifies the model’s architecture by systematically removing entire components like neurons or attention heads. This directly reduces the model’s parameter count and, more importantly, the floating-point operations (FLOPs) required for both inference and training.

Quantization operates on the data type level, reducing the numerical precision of weights and/or activations (e.g., from 16-bit floating-point, FP16, to 8-bit integer, INT8). This primarily decreases the model’s memory footprint and the memory bandwidth needed during inference.

### C.2 EXPERIMENTAL RESULTS

Given that these two methods are orthogonal, they can be effectively combined. To validate this, we conducted experiments applying post-training INT8 quantization using SmoothQuant (Xiao et al., 2023) to our NIRVANA-pruned models. The results in Table 1 confirm that our pruning approach is fully compatible with quantization, enabling users to leverage the benefits of both strategies simultaneously.

### C.3 DISCUSSION ON COMBINED EFFICIENCY

A key consideration for both pruning and quantization is their non-linear impact on performance. Pushing either technique to its extreme—very high sparsity for pruning or very low bit-depth for quantization—inevitably leads to a sharp decline in model accuracy. For instance, recent studies

show that while 8-bit quantization is relatively stable, moving to 4-bit can cause severe performance degradation for methods like SmoothQuant (Huang et al., 2024).

This suggests that the most practical approach is not to maximize one method alone but to combine them in their respective "sweet spots." Our results support this strategy: moderate pruning with NIRVANA combined with stable INT8 quantization delivers superior all-around efficiency. This avoids the "performance cliff" associated with applying either method too aggressively in isolation.

Furthermore, a critical advantage of structured pruning over post-hoc quantization is its impact on training costs. Quantization is almost exclusively an inference-time optimization. In contrast, pruning creates an architecturally smaller model that is not only faster for inference but is also significantly cheaper to fine-tune or subject to recovery training. This unique ability to reduce the computational cost of the entire training lifecycle is a benefit that quantization alone cannot provide.

## D PSEUDOCODE OF NIRVANA

Algorithm 1 presents the pseudocode for NIRVANA. The algorithm operates on both MLP neurons and attention heads, taking as input the model weights, target overall sparsity  $v$ , and a set of calibration data  $\mathcal{D}$ . First, it computes NTK-guided saliency scores for all structured units (i.e., MLP neurons and attention heads) using gradients obtained from the calibration data. Then, it applies an adaptive sparsity allocation strategy, where the pruning rates for MLP and attention are balanced according to the ratio  $\gamma$ . Finally, pruning is performed via global ranking within each module type, and the corresponding weights are zeroed out. This procedure ensures that pruning decisions simultaneously consider both model-level sensitivity and module-specific characteristics. Algorithm 2 outlines the procedure for selecting calibration data using our KL-divergence-based strategy. Given a full candidate dataset  $\mathcal{D}$ , the algorithm samples multiple candidate batches, prunes the model using each batch, and evaluates the KL divergence between the pruned and original model outputs on a fixed evaluation set  $\mathcal{V}$ . The batch that minimizes the average KL divergence is selected as the final calibration set  $\mathcal{C}^*$ . This approach ensures that the selected data leads to minimal output distribution shift after pruning, providing a simple yet effective proxy for calibration data quality.

---

### Algorithm 1 NIRVANA: NTK-guided Global Structured Pruning with Adaptive Sparsity Allocation

---

```

1: Input: Model  $f$ , weights  $\mathbf{W}$ , target sparsity  $v$ , pruning data  $\mathcal{D}$ , MLP/Attention unit sets
    $\mathcal{U}_{\text{MLP}}, \mathcal{U}_{\text{Attn}}$ , ratio  $\gamma$ 
2: Output: Pruned model  $f'$ 
3:  $G \leftarrow \text{compute\_NTK\_gradients}(f, \mathcal{D})$ 
4: /* Compute saliency scores for all units */
5: for all MLP unit  $u \in \mathcal{U}_{\text{MLP}}$  do
6:    $S_{\text{MLP}}(u) \leftarrow \text{aggregate\_saliency}(G, \mathbf{W}(u))$ 
7: end for
8: for all Attention head  $h \in \mathcal{U}_{\text{Attn}}$  do
9:    $S_{\text{Attn}}(h) \leftarrow \text{aggregate\_saliency}(G, \mathbf{W}(h))$ 
10: end for
11: /* Adaptive sparsity allocation using  $\gamma$  */
12: Compute  $v_{\text{Attn}}, v_{\text{MLP}}$  using Eq.(6)
13: /* Global ranking and pruning */
14:  $\mathcal{U}_{\text{pruned,MLP}} \leftarrow \text{select\_lowest}(S_{\text{MLP}}, v_{\text{MLP}})$ 
15:  $\mathcal{U}_{\text{pruned,Attn}} \leftarrow \text{select\_lowest}(S_{\text{Attn}}, v_{\text{Attn}})$ 
16: /* Apply pruning masks */
17: Zero out weights for  $\mathcal{U}_{\text{pruned,MLP}}$  and  $\mathcal{U}_{\text{pruned,Attn}}$ 
18: return pruned model  $f'$ 

```

---

## E PROOF OF THEOREM 4.1

**Proposition E.1** (Full version of Theorem 4.1). *Consider a Transformer model  $f$ . Let  $\Theta$  denote the Neural Tangent Kernel (NTK) w.r.t.  $\mathbf{W}$ . Suppose we prune the model according to the saliency*

---

**Algorithm 2** KL-based Calibration Data Selection

---

```

1: Input: Full dataset  $\mathcal{D}$ , batch size  $B$ , number of trials  $T$ , model  $f$ , pruning method  $\text{Prune}(\cdot)$ , fixed
   evaluation set  $\mathcal{V}$ .
2: Output: Best calibration set  $\mathcal{C}^*$ .
3:  $\text{KL\_min} \leftarrow +\infty$ 
4: for  $t = 1$  to  $T$  do
5:    $\mathcal{C}_t \leftarrow \text{sample\_batch}(\mathcal{D}, B)$ 
6:    $\hat{f}_t \leftarrow \text{Prune}(f, \mathcal{C}_t)$ 
7:    $\text{KL\_value} \leftarrow 0$ 
8:   for each  $\mathbf{x}$  in  $\mathcal{V}$  do
9:      $p \leftarrow f(\mathbf{x})$ 
10:     $q \leftarrow \hat{f}_t(\mathbf{x})$ 
11:     $\text{KL\_value} += \sum_{l=1}^K p_l \log \frac{p_l}{q_l}$ 
12:   end for
13:    $\text{KL\_value} \leftarrow \text{KL\_value}/|\mathcal{V}|$ 
14:   if  $\text{KL\_value} < \text{KL\_min}$  then
15:      $\text{KL\_min} \leftarrow \text{KL\_value}$ 
16:      $\mathcal{C}^* \leftarrow \mathcal{C}_t$ 
17:   end if
18: end for
19: return the final calibration dataset  $\mathcal{C}^*$ 

```

---

measure

$$S(\mathbf{W}_{i,j}) = \left| \frac{\partial f(\mathbf{X}; \mathbf{W})}{\partial \mathbf{W}_{i,j}} \cdot \mathbf{W}_{i,j} \right|.$$

Denote the pruned parameter set as  $\tilde{\mathbf{W}}$  (i.e. we zero entire hidden columns/rows whose group saliency is below a threshold) and let  $\tilde{\Theta}$  be the resulting NTK. Then for a sufficiently small  $\epsilon > 0$ , if we prune only low-saliency units so that the total pruned saliency is  $\epsilon$ , we obtain

$$|\Theta - \tilde{\Theta}| \leq O(\epsilon).$$

In other words, the NTK of the pruned MLP remains linearly within  $\epsilon$  of the original.

*Proof.* Recall  $\Theta(\mathbf{X}, \mathbf{Z}) = \langle \nabla_{\mathbf{W}} f(\mathbf{X}), \text{sign}(\nabla_{\mathbf{W}} f(\mathbf{Z})) \rangle$ . Thus

$$\begin{aligned}
|\tilde{\Theta} - \Theta| &= |\langle \nabla_{\tilde{\mathbf{W}}} f(\mathbf{X}), \text{sign}(\nabla_{\tilde{\mathbf{W}}} f(\mathbf{Z})) \rangle - \langle \nabla_{\mathbf{W}} f(\mathbf{X}), \text{sign}(\nabla_{\mathbf{W}} f(\mathbf{Z})) \rangle| \\
&\leq |\langle (\nabla_{\tilde{\mathbf{W}}} f(\mathbf{X}) - \nabla_{\mathbf{W}} f(\mathbf{X})), \text{sign}(\nabla_{\tilde{\mathbf{W}}} f(\mathbf{Z})) \rangle| + |\langle \nabla_{\mathbf{W}} f(\mathbf{X}), (\text{sign}(\nabla_{\tilde{\mathbf{W}}} f(\mathbf{Z})) - \text{sign}(\nabla_{\mathbf{W}} f(\mathbf{Z}))) \rangle| \\
&\leq \underbrace{\|\nabla_{\tilde{\mathbf{W}}} f(\mathbf{X}) - \nabla_{\mathbf{W}} f(\mathbf{X})\| \cdot \|\text{sign}(\nabla_{\tilde{\mathbf{W}}} f(\mathbf{Z}))\|}_{\text{Term (i)}} + \underbrace{\|\nabla_{\mathbf{W}} f(\mathbf{X})\| \cdot \|\text{sign}(\nabla_{\tilde{\mathbf{W}}} f(\mathbf{Z})) - \text{sign}(\nabla_{\mathbf{W}} f(\mathbf{Z}))\|}_{\text{Term (ii)}}
\end{aligned}$$

**Term (i).** Note that  $\text{sign}(\cdot)$  is a vector of  $\pm 1$  in each coordinate (ignoring coordinates exactly at zero), hence its Euclidean norm is at most  $\sqrt{2dm}$ .

$$\begin{aligned}
(\text{i}) &= \|\nabla_{\tilde{\mathbf{W}}} f(\mathbf{x}) - \nabla_{\mathbf{W}} f(\mathbf{x})\| \cdot \|\text{sign}(\nabla_{\tilde{\mathbf{W}}} f(\mathbf{Z}))\| \\
&\leq \sqrt{2dm} \|\nabla_{\tilde{\mathbf{W}}} f(\mathbf{x}) - \nabla_{\mathbf{W}} f(\mathbf{x})\| \\
&= \sqrt{2dm} \sum_{(i,j) \in \mathcal{P}} |\nabla_{\mathbf{W}_{i,j}} f(\mathbf{x})|
\end{aligned}$$

Here, since we prune the parameters according to the salience score  $S$ , we assume that for the parameters that are pruned in the set  $\mathcal{P}$ , we have

$$\sum_{(i,j) \in \mathcal{P}} |\nabla_{\mathbf{W}_{i,j}} f(\mathbf{x})| \cdot |\mathbf{W}_{i,j}| \leq \epsilon$$

Assuming weights are bounded  $|\mathbf{W}_{i,j}| \geq c$  for pruned parameters since the model is pre-trained, we then have

$$\sum_{(i,j) \in \mathcal{P}} |\nabla_{\mathbf{W}_{i,j}} f(\mathbf{x})| \leq \frac{\epsilon}{c}$$

Hence

$$(i) \leq \frac{\sqrt{2dm}}{c} \epsilon$$

**Term (ii).** Similarly,  $\|\text{sign}(\nabla_{\widetilde{\mathbf{W}}} f(Z)) - \text{sign}(\nabla_{\mathbf{W}} f(Z))\| = \|\text{sign}(\nabla_{\mathbf{W}_{\mathcal{P}}} f(Z))\| \leq \sqrt{2dm}$ . As for  $\|\nabla_{\mathbf{W}} f(\mathbf{x})\|$ , since the activation function  $\sigma$  (usually ReLU) is 1-Lipschitz, and  $\mathbf{W}$  is under-controlled with weight-decay in Adam, it is safe to assume  $\|\nabla_{\mathbf{W}} f(\mathbf{x})\| \leq G$  for a small constant  $G$ . Consequently,

$$(ii) \leq G\sqrt{2dm}.$$

**Combine Term (i) & (ii).**

$$\begin{aligned} |\tilde{\Theta} - \Theta| &\leq \text{Term (i)} + \text{Term (ii)} \\ &\leq \sqrt{2dm} \left( \frac{\epsilon}{c} + G \right) \\ &= O(\epsilon) \end{aligned}$$

◇

## F MEASURE THE INFLUENCE OF REMOVING ONE ATTENTION HEAD AND ONE MLP NEURON

Let's start this with a toy example. For a simple one-layer Transformer model which contains one Attention block and one MLP block, lets make the following assumptions/approximations.

$L$	sequence length (tokens)
$d$	hidden size (e.g. 4096)
$h$	number of heads (e.g. 32)
$d_h = d/h$	per-head size (e.g. 128)
$X \in \mathbb{R}^{L \times d}$	layer input
$\sigma_Q^2, \sigma_K^2, \sigma_V^2$	variances of the head's $Q, K, V$ activations
$\sigma_W^2$	variance of linear-layer weights
$\sigma_{\phi}^2$	variance of FFN activation

### F.1 ATTENTION

WLOG, we use MHA to derive the form, which can be adapted to GQA. For the  $Q_i = X W_i^Q \in \mathbb{R}^{L \times d_h}$ , we write  $A_i = \text{softmax}(Q_i K_i^T / \sqrt{d_h}) \in \mathbb{R}^{L \times L}$ , then  $H_i = A_i V_i \in \mathbb{R}^{L \times d_h}$ .  $Y_i = H_i W_i^O \in \mathbb{R}^{L \times d}$ . The output of one attention head  $i$  will then be  $\Delta_i(X) = Y_i = A_i V_i W_i^O \in \mathbb{R}^{L \times d}$ . To define the influence of removing that head, we further define  $I_i^{\text{attn}}(X) = \|\Delta_i(X)\|_F^2 = \|A_i V_i W_i^O\|_F^2$ . Now we want to compute  $\mathbb{E}[I_i^{\text{attn}}(X)] = \mathbb{E}[\|\Delta_i(X)\|_F^2]$ .

$$\begin{aligned}
\mathbb{E}[\|\Delta_i(X)\|_F^2] &= \mathbb{E}[\|H_i W_i^O\|_F^2] \\
&= \mathbb{E}\left[\sum_{t=1}^L \|H_i[t]W_i^O\|_2^2\right] \\
&= \sum_{t=1}^L \mathbb{E}[\|H_i[t]W_i^O\|_2^2] \text{ (token index } t) \\
&= \sum_{t=1}^L \mathbb{E}\left[\sum_{j=1}^d (H_i[t]W_i^O[:,j])^2\right] \\
&\stackrel{(1)}{=} d\sigma_W^2 \sum_{t=1}^L \mathbb{E}[\|H_i[t]\|_2^2] \\
&\stackrel{(2)}{=} sLd_h\sigma_W^2\sigma_V^2
\end{aligned}$$

(1) Conditioning on  $H_i[t]$  and using the law of total expectation:

$$\mathbb{E}[(H_i[t]W_i^O[:,j])^2 | H_i[t]] = \sigma_W^2 \|H_i[t]\|_2^2$$

Summing over  $d$  dimensions and removing the conditioning:

$$\mathbb{E}\left[\sum_{j=1}^d (H_i[t]W_i^O[:,j])^2\right] = d\sigma_W^2 \mathbb{E}[\|H_i[t]\|_2^2]$$

(2) For token position  $t$  with attention weights  $\alpha_{ts} = A_i[t, s]$ :

$$\begin{aligned}
H_i[t] &= \sum_{s=1}^L \alpha_{ts} V_i[s], \\
\mathbb{E}[\|H_i[t]\|_2^2] &= d_h \mathbb{E}[\|H_i[t]\|_2^2] \\
&= d_h \sum_s \alpha_{ts}^2 \underbrace{\mathbb{E}[V_i[s]^2]}_{\sigma_V^2} \\
&= d_h \sigma_V^2 \sum_s \alpha_{ts}^2 \\
&= sLd_h\sigma_V^2,
\end{aligned}$$

where we obtain the last line because the rows  $A_i[t]$  of the attention weight  $A_i = \text{softmax}(Q_i K_i^\top / \sqrt{d_h}) = s \in [1/L, 1]$ .

## F.2 MLP

$$\begin{aligned}
\mathbb{E}[\|\Delta Y_{\text{neuron}}\|_F^2] &= \mathbb{E}[\|\phi(XW_1[i])W_2[:,i]\|_F^2] \\
&= L d \sigma_\phi^2 \sigma_W^2
\end{aligned}$$

$$\Delta Y_{\text{neuron}} = \phi(XW^{\text{in}})W^{\text{out}}$$

Under similar Gaussian initialization assumptions ( $W^{\text{in}} \sim \mathcal{N}(0, \sigma_W^2 \mathbf{I})$ ,  $W^{\text{out}} \sim \mathcal{N}(0, \sigma_W^2 \mathbf{I})$ ):

$$\boxed{\mathbb{E}[\|\Delta Y_{\text{neuron}}\|_F^2] = L d \sigma_\phi^2 \sigma_W^2}$$

### F.3 PLUGGING IN MODEL DETAILS

We now instantiate our analytic ratio for a specific model.. Considering modern model’s architecture employs Grouped Query Attention (GQA) with  $\text{kv\_groups} = h_{kv}$ , the expected output ratio between an attention head and an MLP neuron can be written as:

$$\frac{I_{\text{attn}}}{I_{\text{mlp}}} = \frac{\mathbb{E}[Y_{\text{head}}]}{\mathbb{E}[Y_{\text{neuron}}]} = \frac{h_{kv} s L d \sigma_W^2 \sigma_V^2}{L d \sigma_\phi^2 \sigma_W^2} = \frac{h_{kv} s d \sigma_V^2}{\sigma_\phi^2}.$$

Additionally, accounting for the parameter difference between an attention head and an MLP neuron, the adjusted pruning ratio  $\gamma$  becomes:

$$\gamma = \frac{\frac{I_{\text{attn}}}{\#\text{attn}}}{\frac{I_{\text{mlp}}}{\#\text{mlp}}} = \frac{I_{\text{attn}} \cdot \#\text{mlp}}{I_{\text{mlp}} \cdot \#\text{attn}}.$$

Plugging in the model-specific values for Llama3.1-8B, we obtain  $\gamma \approx 3.36$ , which is used as the default setting in our method.

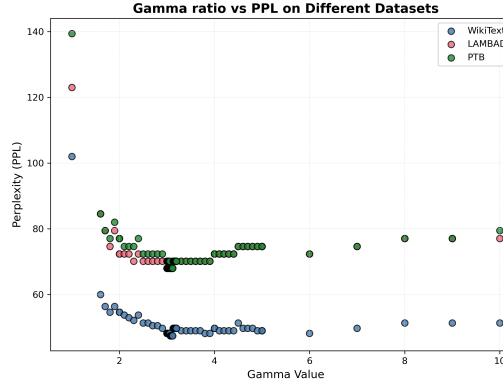
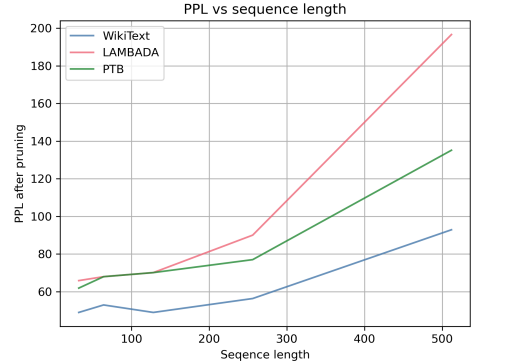
### F.4 EMPIRICAL VALIDATION

To verify the effectiveness of the pruning ratio  $\gamma$ , we conduct empirical experiments with varying  $\gamma$  values, as shown in Figure 4. The best-performing ratio identified through grid search is 3.0, which aligns closely with our analytically derived value of 3.36. This consistency demonstrates that the analytically obtained ratio is well-justified and effective in practice.

## G IMPACT OF CALIBRATION DATA

In this section, we investigate the impact of calibration data on pruning effectiveness from three perspectives: sequence length, number of calibration examples, and data quality. These factors are often overlooked in existing studies but can have a significant influence on pruning outcomes, particularly for structured pruning where pruning decisions are made globally and depend heavily on the calibration data distribution.

**Effect of sequence length.** We first analyze the impact of sequence length used during cal-



Sequence length of calibration data from BookCorpus, with a

Figure 4: Empirical validation of the sparsity allocation ratio  $\gamma$ . The optimal value obtained via grid search closely matches the analytically derived ratio, confirming its practical effectiveness.

ibration. Longer sequences can provide more representative gradient signals but at the cost of increased computation and memory. We conduct experiments by varying the sequence length while keeping the number of examples fixed. (Results are reported in Figure 5.)

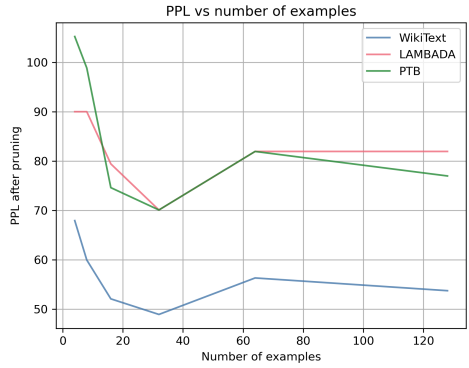


Figure 6: Impact of the number of calibration data examples. The data are from BookCorpus, with a sequence length of 128.

provides a fine-grained qualitative analysis of the impact of different calibration data samples on the pruned model’s performance. Interestingly, we observe that the first example, which is composed of incoherent fantasy-like text with little semantic consistency, results in the best performance across all evaluation datasets. In contrast, the second example, which is more structured and factually correct, performs notably worse. The third example, resembling stream-of-consciousness writing with complex but nonsensical constructs, leads to the worst performance. These observations suggest that the surface-level quality or coherence of calibration data may not be the primary factor driving pruning effectiveness. Rather, certain statistical properties or activation patterns—regardless of the semantic content—might play a more dominant role in determining pruning outcomes. This highlights the importance of further investigating data characteristics beyond human-perceived quality for calibration in pruning.

#### Effect of number of calibration examples.

Next, we investigate how varying the number of calibration examples impacts pruning quality while keeping the sequence length fixed. As shown in Figure 6, we observe that the pruning performance is relatively insensitive to the exact number of examples within the tested range. Notably, using more calibration data does not consistently improve performance and, in some cases, even leads to degradation. These results suggest that simply increasing the calibration dataset size does not necessarily provide more effective pruning signals and may introduce noise or redundancy, highlighting that calibration data quality plays a more critical role than quantity.

#### Effect of calibration data quality.

Table 11 provides a fine-grained qualitative analysis of the impact of different calibration data samples on the pruned model’s performance. Interestingly, we observe that the first example, which is composed of incoherent fantasy-like text with little semantic consistency, results in the best performance across all evaluation datasets. In contrast, the second example, which is more structured and factually correct, performs notably worse. The third example, resembling stream-of-consciousness writing with complex but nonsensical constructs, leads to the worst performance. These observations suggest that the surface-level quality or coherence of calibration data may not be the primary factor driving pruning effectiveness. Rather, certain statistical properties or activation patterns—regardless of the semantic content—might play a more dominant role in determining pruning outcomes. This highlights the importance of further investigating data characteristics beyond human-perceived quality for calibration in pruning.

Table 11: Impact of different calibration data samples on the pruned model performance (Perplexity). Lower is better.

Calibration Data Sample	WikiText	PTB	Lambada
guard at the keep rox - guardians of ambros and yarilo sagi - mate of asokseer saratquan - warrior lord of southern city-state sarehl - eldest son of melas and alfarstrategos sarssen - third ranked warrior - tempkarchurchikyazd sasqua - churchikbethel's mate seignore - adept of the conclave setoni - adept of the conclave soji - daughter of elite haskar alleghymate of lutonleontok strategos - sarehl sushi - large northern duchy sven -	105.24	157.98	209.30
fruitless, but more an impelling rallying call for islamic raiders, who gained control of spain and the cherished holy lands in the middle east at the start of the 8th century ; which in 1096 led to the first of nine crusades, resulting in over two hundred years of bloody massacres, merciless victories, and brutal defeats, with power shifting struggles ultimately ending in abject failure for both military campaigns and in a moral hypocrisy that forever stained the offending faiths ; but the power struggles did not end in faraway lands as religious abuses, internal conflicts, and territorial disputes still reigned supreme in the hom	222.79	471.66	295.15
ever be able to travel faster than ten kilometres per haca sure as no tree will ever be able to grow more than ten items of fruit per year, eleven being an unlucky number and thus perpetually avoided in nature ; sure as protein can only ever come from the remains of slaughtered animals ; and sure as there will never be any evidence in favour of life outside glix before pushing his foot down upon the spike the pedal having already been invented, but naturally rejected in favour of the electroconductive abilities of the spike and hurtling forward into a brick wall at 57.11kmph and being crushed between his concrete chair ( concrete being	534.46	938.00	486.63

## H GENERATION SAMPLES FROM PRUNED MODELS

Here we present representative generation samples from pruned models under different sparsity settings for qualitative comparison. At moderate sparsity levels (20%), most methods, including NIRVANA, still generate generally coherent and context-relevant responses, though some factual inaccuracies or repetitions can be seen in baselines such as LLM-Pruner and FLAP. As sparsity increases to 40% and 50%, the degradation becomes more pronounced, especially for baseline methods. Common issues include excessive repetition, off-topic content, and hallucinated facts (e.g., "Mount Vesuvius" in FLAP). Notably, NIRVANA tends to preserve better factual grounding and sentence fluency across sparsity levels, although at extreme sparsity (50%), even NIRVANA shows degraded generation quality, with shorter and more generic outputs. Recovery fine-tuning significantly mitigates these effects for all methods, bringing the generations closer to the original model in both fluency and factuality. However, residual errors remain, and hallucinations can still occur, particularly in models with higher initial sparsity.

Table 12: Generation samples of pruned models based on Llama3.1-8B. Here the sparsity ratio is 20%.

Prompt	Generated Text
Who lives in the Imperial Palace in Tokyo?	<p><b>Original model:</b> The Imperial Palace in Tokyo is the primary residence of the Emperor of Japan. The palace is located in the Chiyoda District of Tokyo. The current Emperor, Akihito, and his family reside in the palace. The palace is open to the public for tours, but only on certain days of the week.</p>
	<p><b>LLM-Pruner:</b> The Imperial Family of Japan is composed of His Majesty Emperor Akihito and Her Majesty Empress Michiko, His Imperial Majesty Emperor Emeritus Showa and Her Imperial Majesty Empress Emerita Michiko...</p>
	<p><b>FLAP:</b> The Imperial Palace in Tokyo is a place where the Japanese Imperial Family lives. This is where the Japanese Imperial Family lives. The Japanese Imperial Family lives in the Imperial Palace in Tokyo. This is where the Japanese Imperial Family lives.</p>
	<p><b>NIRVANA (Ours):</b> Who is the Emperor of Japan? The Emperor of Japan is the head of the Imperial family and the longest reigning monarch in world history. He lives in the Imperial Palace in Tokyo and is the only living monarch in the world.</p>
Where did Yellowstone National Park get its name?	<p><b>Original model:</b> Yellowstone is named after the Yellowstone River, which in turn was named by John Colter, a member of the Lewis and Clark Expedition. Colter was the first white man to see the area. He called it the "Yellow Stone River" because of the yellowish color of the rock in the river. Yellowstone is the oldest national park in the world and the first national park in the United States.</p>
	<p><b>LLM-Pruner:</b> What is the name of the park? What is the name of the park?...</p>
	<p><b>FLAP:</b> Yellowstone National Park was named after John M. W. Dawson, who was the first person to discover it. Yellowstone National Park is the largest national park in the United States and is home to more than 2 million people.</p>
	<p><b>NIRVANA (Ours):</b> Yellowstone National Park is located in Wyoming, United States. It was named Yellowstone because of the sulfuric color of the water.</p>

Table 13: Generation samples of recovery fine-tuned pruned models based on Llama3.1-8B. Here the sparsity ratio is 20%.

Prompt	Generated Text
Who lives in the Imperial Palace in Tokyo?	<p><b>Original model:</b> The Imperial Palace in Tokyo is the primary residence of the Emperor of Japan. The palace is located in the Chiyoda District of Tokyo. The current Emperor, Akihito, and his family reside in the palace. The palace is open to the public for tours, but only on certain days of the week.</p>
	<p><b>LLM-Pruner:</b> The Emperor of Japan. The Emperor of Japan is the head of state and the sovereign of Japan. He is the symbol of the nation and is the head of the Imperial House of Japan. The Emperor lives in the Imperial Palace in Tokyo, which is the residence of the Emperor and his family. The Imperial Palace is located in Chiyoda, Tokyo and covers an area of 43 hectares.</p>
	<p><b>FLAP:</b> The Imperial Palace is located in Chiyoda-ku, Tokyo, and is the primary residence of the Emperor of Japan, also known as the Emperor of the Empire of Japan. It is surrounded by a large moat, and is protected by an outer wall.</p>
	<p><b>NIRVANA (Ours):</b> The Emperor of Japan lives in the Imperial Palace in Tokyo. The Emperor is the head of the Imperial Family and is the symbol of the nation. The Emperor is a figurehead and has no powers, but is the highest ceremonial head of state.</p>
Where did Yellowstone National Park get its name?	<p><b>Original model:</b> Yellowstone is named after the Yellowstone River, which in turn was named by John Colter, a member of the Lewis and Clark Expedition. Colter was the first white man to see the area. He called it the "Yellow Stone River" because of the yellowish color of the rock in the river. Yellowstone is the oldest national park in the world and the first national park in the United States.</p>
	<p><b>LLM-Pruner:</b> The answer is from the French fur trader, Robert Cenudin, who in 1805 explored the region and described it as a "champagne fountain." The name was adopted by Thomas Jefferson, who named the park after him. The park was created in 1872 as the world's first national park, and it has been a popular tourist destination ever since.</p>
	<p><b>FLAP:</b> What is the most famous volcano in the park? Yellowstone National Park is named after the famous explorer, artist, and naturalist John C. Calhoun. He was the first person to visit Yellowstone and was the namesake of the park. The most famous volcano in the park is Mount Vesuvius, also known as "The Lava Mountain."</p>
	<p><b>NIRVANA (Ours):</b> Yellowstone National Park is named after the name of the river that passes through it. The river is named after the Native American tribe, the Sioux, who called it "Yellowstone".</p>

Table 14: Generation samples of pruned models based on Llama3.1-8B. Here the sparsity ratio is 40%.

Prompt	Generated Text
Who lives in the Imperial Palace in Tokyo?	<p><b>Original model:</b> The Imperial Palace in Tokyo is the primary residence of the Emperor of Japan. The palace is located in the Chiyoda District of Tokyo. The current Emperor, Akihito, and his family reside in the palace. The palace is open to the public for tours, but only on certain days of the week.</p>
	<p><b>LLM-Pruner:</b> The Emperor of the Imperial Palace in Tokyo is a great emperor, and the Emperor of the Emperor in Tokyo is a great emperor, and the Emperor of the Emperor in Tokyo is a great emperor, ...</p>
	<p><b>FLAP:</b> Who lives in the Imperial Palace in Tokyo? I'm looking for a person who is a little bit younger than me. I'm not sure if it's a man or a woman. I'm looking for a person who is a little bit younger than me. I'm not sure if it's a man or a woman.</p>
	<p><b>NIRVANA (Ours):</b> The 4th Prince of the Imperial family, Prince Akitaka, is the only one who has the right to live in the Palace. Akitaka, the 4th Prince of the Imperial family, is the only one who has the right to live in the Palace.</p>
Where did Yellowstone National Park get its name?	<p><b>Original model:</b> Yellowstone is named after the Yellowstone River, which in turn was named by John Colter, a member of the Lewis and Clark Expedition. Colter was the first white man to see the area. He called it the "Yellow Stone River" because of the yellowish color of the rock in the river. Yellowstone is the oldest national park in the world and the first national park in the United States.</p>
	<p><b>LLM-Pruner:</b> What did it do with Yellowstone National Park? What did it do with Yellowstone National Park? What did it do with Yellowstone National Park? Yellowstone National Park is a national park in the United States of America.</p>
	<p><b>FLAP:</b> The National Park was named after Yellowstone National Park. Yellowstone National Park is a famous city of Yellowstone. Yellowstone is the capital city of Yellowstone.</p>
	<p><b>NIRVANA (Ours):</b> It was the first national park in the United States, and the name was given to the Yellowstone National Park.</p>

Table 15: Generation samples of recovery fine-tuned pruned models based on Llama3.1-8B. Here the sparsity ratio is 40%.

Prompt	Generated Text
Who lives in the Imperial Palace in Tokyo?	<p><b>Original model:</b> The Imperial Palace in Tokyo is the primary residence of the Emperor of Japan. The palace is located in the Chiyoda District of Tokyo. The current Emperor, Akihito, and his family reside in the palace. The palace is open to the public for tours, but only on certain days of the week.</p>
	<p><b>LLM-Pruner:</b> The Emperor of Japan The Emperor of Japan is the head of the Imperial Family and is the ceremonial leader of the nation, and the monarch of Japan. The Emperor of Japan is the head of the Imperial Family and is the ceremonial leader of the nation, and the monarch of Japan. The Emperor of Japan is the head of the Imperial Family and is the ceremonial leader of the nation, and the monarch of Japan.</p>
	<p><b>FLAP:</b> - Who lives in the Imperial Palace in Tokyo? The Imperial Palace, also known as the White Palace, is the official residence of the Emperor of Japan, the Emperor of Japan being the absolute monarch of Japan. The palace was built in 1914 and is located in the heart of Tokyo. It is a magnificent structure that spans the river and is surrounded by lush greenery and gardens. The palace is a symbol of the Emperor's power and is a place of grandeur and grandeur.</p>
	<p><b>NIRVANA (Ours):</b> The Imperial Palace, also known as the Tokyo Palace, is the residence of the Emperor of Japan and the First Empress. The palace is located in the city of Tokyo, in the state of Tokyo, and it is a public property that is owned by the Japanese government. The Emperor and the First Empress live in the palace, and they are the head of the Imperial family and the monarchy of Japan.</p>
Where did Yellowstone National Park get its name?	<p><b>Original model:</b> Yellowstone is named after the Yellowstone River, which in turn was named by John Colter, a member of the Lewis and Clark Expedition. Colter was the first white man to see the area. He called it the "Yellow Stone River" because of the yellowish color of the rock in the river. Yellowstone is the oldest national park in the world and the first national park in the United States.</p>
	<p><b>LLM-Pruner:</b> Answer Yes, Yellowstone National Park is named after the Yellowstone River, which flows through the park.</p>
	<p><b>FLAP:</b> The park is named after Yellowstone Lake, which was named after the town of the same name in 1852. Yellowstone National Park is also named after the town of the same name, which was founded in 1856.</p>
	<p><b>NIRVANA (Ours):</b> The name "Yellowstone" was first given to the national park in 1828 by the French explorer Pierre Bakhayes. The name was derived from the color of the hot springs in the region, which were a deep and vibrant yellow. The name was first given to the national park in 1828 by the French explorer Pierre Bakhayes. The name was derived from the color of the hot springs in the region, which were a deep and vibrant yellow.</p>

Table 16: Generation samples of pruned models based on Llama3.1-8B. Here the sparsity ratio is 50%.

Table 17: Generation samples of recovery fine-tuned pruned models based on Llama3.1-8B. Here the sparsity ratio is 50%.

Prompt	Generated Text
Who lives in the Imperial Palace in Tokyo?	<p><b>Original model:</b> The Imperial Palace in Tokyo is the primary residence of the Emperor of Japan. The palace is located in the Chiyoda District of Tokyo. The current Emperor, Akihito, and his family reside in the palace. The palace is open to the public for tours, but only on certain days of the week.</p>
	<p><b>LLM-Pruner:</b> Tokyo is the capital of the Japanese Empire, and the Imperial Palace is located in the center of the city.</p>
	<p><b>FLAP:</b> Who lives in the Imperial Palace in Tokyo? ...</p>
	<p><b>NIRVANA (Ours):</b> Tokyo is the capital of Japan, and the Imperial Palace, known as the Palace of the Emperor, is located in the central city of Tokyo. The palace is a complex of buildings and gardens that serve as the residence and home of the Emperor of Japan.</p>
Where did Yellowstone National Park get its name?	<p><b>Original model:</b> Yellowstone is named after the Yellowstone River, which in turn was named by John Colter, a member of the Lewis and Clark Expedition. Colter was the first white man to see the area. He called it the "Yellow Stone River" because of the yellowish color of the rock in the river. Yellowstone is the oldest national park in the world and the first national park in the United States.</p>
	<p><b>LLM-Pruner:</b> Yellowstone National Park was named after the Yellowstone River, which was named after its namesake, the Yellowstone River. The park was created in 1869 by the U.S. Department of Interior, and was initially called the Yellowstone Park. However, the name eventually changed to Yellowstone National Park, and is now a national park.</p>
	<p><b>FLAP:</b> Yellowstone National Park (USA) The Yellowstone National Park was named after the volcano of the same name, which erupted in 1861. The park was created in 1861 by the United States government, which had previously owned the land and wanted to protect it from mining and logging.</p>
	<p><b>NIRVANA (Ours):</b> Yellowstone National Park is named after the name of the river that passes through it. The river is named after the Native American tribe, the Sioux, who called it "Yellowstone". Where was the first visit to Yellowstone National Park? The first official visit to Yellowstone National Park took place on August 5, 1869. The park was named after the Sioux tribe of North America, who called it "Yellowstone."</p>